FEBS Letters

FEBS PRESS science publishing by scientists

Starch biosynthesis by AGPase, but not starch degradation by BAM1/3 and SEX1, is rate-limiting for CO_2-regulated stomatal movements under short-day conditions

Tamar Azoulay-Shemer[1,†], Nikki Schwankl[1], Ido Rog[2], Menachem Moshelion[3] and Julian I. Schroeder[1]

1 Division of Biological Sciences, Cell and Developmental Biology Section, University of California San Diego, La Jolla, CA, USA
2 Department of Plant & Environmental Sciences, Weizmann Institute of Science, Rehovot, Israel
3 The Robert H. Smith Institute of Plant Sciences and Genetics in Agriculture, The Robert H. Smith Faculty of Agriculture, Food and Environment, The Hebrew University of Jerusalem, Rehovot, Israel

Correspondence
J. I. Schroeder, Division of Biological Sciences, Cell and Developmental Biology Section, University of California San Diego, La Jolla, CA 92093-0116, USA
Fax: +1 858 534 7108
Tel: +1 858 534 7759
E-mail: jischroeder@ucsd.edu

[†]Present address
The Robert H. Smith Institute of Plant Sciences and Genetics in Agriculture, The Robert H. Smith Faculty of Agriculture, Food and Environment, The Hebrew University of Jerusalem, Rehovot, Israel

(Received 5 July 2018, revised 10 July 2018, accepted 11 July 2018, available online 10 August 2018)

doi:10.1002/1873-3468.13198

Edited by Ulf-Ingo Flügge

Starch in guard cells functions in osmoregulation during stomatal movements. Starch metabolism is controlled by the circadian clock. We investigated the role of starch metabolism in stomatal responses to CO_2 under different photoperiodic conditions. Guard cell starch levels correlate with low/high [CO_2] exposure. Starch biosynthesis-deficient *AGPase* (*ADG1*) mutants but, unexpectedly, not the starch degradation-deficient BAM1, BAM3, and SEX1 mutants alone, are rate-limiting for stomatal conductance responses to [CO_2]-shifts. Interestingly, *AGPase* is rate-limiting solely under short- but not long-day conditions. These findings suggest a model of enhanced AGPase activity in guard cells under short days such that starch biosynthesis becomes rate-limiting for CO_2-induced stomatal closing.

Keywords: *Arabidopsis*; gas exchange; guard cell; photoperiod; starch synthesis; starch degradation

Starch is an end product of CO_2 assimilation and accumulates in both mesophyll and guard cells. In the mesophyll, the primary photosynthetic tissue, starch accumulates as a temporary store during the day and then remobilizes during the night [1,2]. Starch metabolism provides carbohydrates and supports leaf metabolism, and enables the continued synthesis and export of sucrose [3]. On the other hand, guard cell starch content is linked to stomatal aperture [4] and studies have shown starch metabolism in guard cells to be involved in stomatal conductance regulation [5].

During the day, CO_2 assimilates are partitioned to both starch synthesis in the chloroplast and sucrose synthesis in the cytosol. *Arabidopsis* typically partitions 30–50% of its photoassimilates into insoluble starch granules [2,6,7]. Briefly, fructose 6-phosphate is converted to glucose 1-phosphate (Glc1P) by the serial action of phosphoglucoisomerase (PGI) and

Abbreviations
AGPase, ADP-glucose pyrophosphorylase (also referred as ADGase); BAM, β-amylase; GWD also termed SEX1, Plastidial glucan water dikinase; LD, long day 16 h light/8 h dark; MD, medium length day 12 h light/12 h dark; SD, short day 8 h light/16 h dark.

phosphoglucomutase (PGM1), which is then converted to ADP-glucose by the enzyme ADP-glucose pyrophosphorylase (AGPase, also referred as ADGase), consuming ATP and releasing inorganic pyrophosphate (PPi). This last step produces the glucosyl donor for starch synthesis and is considered to be a rate-limiting and committed step for starch biosynthesis. *Arabidopsis* mutants in which PGI, PGM, or AGPase activities are reduced or abolished, show reduced leaf starch levels [8–10].

On the other hand, during the night, starch is degraded in mesophyll chloroplasts to produce maltose and glucose, which are then exported to the cytosol for further metabolism [7,11]. The initial step in starch degradation is the phosphorylation of the amylopectin chains by phosphoglucan, water dikinases (PWD), and the plastidial glucan water dikinase (GWD). The GWD enzyme, also named SEX1 (starch excess1) is required for normal β-amylase-mediated leaf starch mobilization [12,13]. Plants lacking key starch degradation enzymes, as SEX1 and some isoforms of the β-amylase enzymes (BAMs), develop starch-excess phenotypes [12,14,15].

Starch metabolism is regulated differently in mesophyll and guard cells [4]. It has been shown that guard cells maintain high starch concentrations during the night [16] and rapidly degrade starch upon illumination [3,17]. Ogawa [18] showed similar stomatal conductance responses to blue light when comparing the starch-containing guard cells of *Vicia faba* and the starch-deficient guard cells of *Alium cepa*. *Allium cepa* was shown to compensate for the lack of starch in guard cells by taking up chloride ions as counter ion to potassium ions rather than relying on malate ions that are produced *via* starch degradation in most guard cells [19,20]. Studies have demonstrated that blue light signaling triggers starch degradation in guard cells [17,18,21], and this degradation contributes to blue light-induced stomatal conductance regulation [17].

The expression pattern of key starch metabolic enzymes differs in mesophyll and in guard cells. The expression level of the starch biosynthesis enzyme *AGPase* expression shows ~4.5 times higher transcript levels in guard cells than mesophyll cells [22] Tissue-specific specialization of isozymes in various gene families has been found. For example, *BAM3* is preferentially expressed in the mesophyll, whereas the ADP-glucose pyrophosphorylase large subunits, *APL3* and *APL4* are preferentially expressed in guard cells [22–24]. Furthermore, β-amylase isozymes have been shown to specialize in a tissue-specific manner: BAM3 is the main β-amylase of *Arabidopsis* leaves, and *bam3* mutants display robust starch overaccumulation in leaves [25]. In contrast, BAM1 is involved in guard cell starch catabolism, and *bam1* mutants show starch excess in guard cells [17,26]. Together, these observations suggest tissue-specific regulation of starch metabolism.

The CO_2 concentration in the intercellular spaces in leaves (C_i) rapidly rises in response to darkness due to respiration and C_i rapidly falls in response to light due to photosynthesis [27]. C_i elevations cause closing of stomatal pores and C_i reduction causes opening of stomatal pores [28]. Furthermore, the continuing rise in the atmospheric CO_2 concentration causes a rise in C_i and thus a reduction in stomatal pore apertures on a global scale [29,30]. Guard cell starch metabolism is involved in stomatal conductance regulation. Starch breakdown was previously shown during stomatal opening, in response to blue light [16,17,21,31,32] or low CO_2 [3,33]. Starch synthesis occurs during stomatal closure in response to drought and abscisic acid [34]. Briefly, during stomatal opening starch is suggested to be degraded to sugars [35–37] and malate [38–40], which are osmotically active solutes that contribute to stomatal opening. However, time-resolved CO_2-regulated stomatal conductance changes have not yet been investigated in starch degradation mutants. During stomatal closure, guard cells can dispose of malate and sugars by metabolism, starch biosynthesis and malate efflux [4,41,42]. Sugars and malate are also imported from the mesophyll and play a role in stomatal conductance regulation [43–45].

ADP-glucose pyrophosphorylase (AGPase) is a key enzyme in starch biosynthesis, controlling starch levels [1,46]. A role for AGPase in high CO_2-induced stomatal closure has been characterized [47]. Starch-deficient *Arabidopsis* mutants in the *AGPase* small subunit (*adg1-1* and *aps1*) contain less than 3% wild-type starch levels in all plant tissues [9,48,49]. In contrast, the plastidial phosphoglucose isomerase (*pPGI*) mutant (*pgi1-1*) retains starch accumulation in guard cells but is extremely starch-deficient in mesophyll cells [10,50,51]. Analyses of these mutants revealed that under a 12 h light/12 h dark growth cycle, stomatal conductance responses to high CO_2 are impaired in *AGPase* mutant plants [47]. However, stomata of *pPGI* mutant plants, that greatly reduce starch levels in mesophyll cells, but not in guard cells, responded to CO_2 changes like wild-type plants [47]. These findings suggest that starch biosynthesis in guard cells but not in mesophyll tissues is involved in CO_2-induced stomatal closing. However, it remained unknown whether starch levels directly modulate stomatal conductance responses to CO_2 shifts, or whether resulting changes in metabolites caused this CO_2 response phenotype.

Furthermore, the effects of starch degradation mutants on CO_2-regulated stomatal movements have not yet been analyzed.

Starch metabolism is controlled by the circadian clock [52–55]. During day, plants regulate partitioning of their total photoassimilates into either sucrose or starch. To meet the carbon demands of the plant during the night, photoperiodic day length affects net daily photosynthesis and starch metabolism [56,57]. Interestingly, the circadian clock was also found to be involved in stomatal conductance regulation [55,58–60]; however, whether photoperiod affects stomatal conductance responses to CO_2 *via* starch metabolism, remains unknown.

In the present study, we investigated CO_2 regulation of stomatal conductance in starch biosynthesis and degradation mutants, and have conducted analyses under three photoperiodic conditions. Unexpectedly, analyses of key starch degradation mutants, which possess a starch-excess phenotype in mesophyll and in guard cells (*bam1bam3*, *sex1-1*) or solely in guard cells (*bam1*), showed intact wild-type-like stomatal responses to CO_2 shifts under all three photoperiodic growth conditions. On the other hand, *AGPase* mutants showed an impaired high CO_2-induced stomatal closing response compared to wild-type plants under short-day (SD: 8 h light/16 h dark), but interestingly not under long-day (LD: 16 h light/8 h dark) photoperiodic growth conditions. Our findings demonstrate that starch biosynthesis mediated by *AGPase*, but not starch degradation mediated solely by BAM1, BAM3, or SEX1 are rate-limiting for stomatal conductance responses to [CO_2] shifts. Furthermore, our study reveals that photoperiod length dramatically affects stomatal conductance responses to high CO_2.

Materials and methods

Plant material

Experiments in this study used the *Arabidopsis thaliana* accession Columbia (Col-0) as wild-type, unless stated otherwise. The following mutants were investigated: two mutant alleles of the ADP-glucose pyrophosphorylase small subunit (*ADG1* AT5G48300): the EMS mutation *adg1-1* [9] and the exon T-DNA insertion *aps1* (SALK_040155) [48], the chloroplast beta-amylase *bam1* mutant (SALK_039895), the *bam1 bam3* double mutant (CS92461 × CS210) [61], and the *starch-excess1 (sex1)* mutant (EMS mutation in AT1G10760) [12].

The T-DNA insertion line *aps1* (SALK_040155) was obtained from the ABRC and genotyped [47]. The *bam1* (SALK_039895) and *bam1 bam3* were kindly provided by Samuel C. Zeeman, and were genotyped using the protocol described by Fulton *et al.* [61]. The *sex1* (EMS mutation) was genotyped by PCR amplification of the DNA fragment containing the gene, using wild-type (Col-0) and the corresponding *Arabidopsis* mutant (*sex1-1*) genomic DNA as templates [12]. PCR was conducted using the following primers: SEX1_For 5′- TCGAAATGGAACGAGAGAGCATAC-3′, SEX1_Rev 5′-CTGCACCTGCATAACCTTCAAGAT-3′, The PCR product was purified and sequenced using SEX1_-seq_Rev 5′-GTACCAGAGGCGAATCAAGGTT-3′, and compared to wild-type.

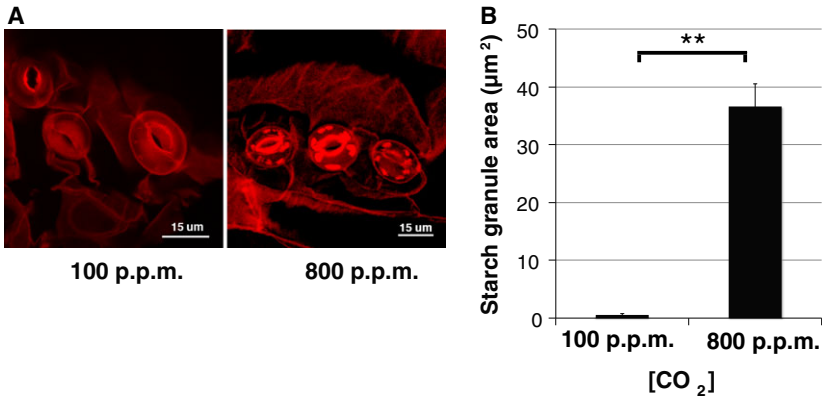

Fig. 1. Starch levels in guard cells of *Arabidopsis* WT leaves following exposure to 45 min of low or high CO_2. *Arabidopsis* WT plants, grown under short-day (SD) conditions, were exposed to low (100 p.p.m.) or high (800 p.p.m.) CO_2 for 45 min. Leaf epidermal peels extracted directly from intact plants were sampled immediately after these CO_2 exposures, and subjected to pseudo-schiff starch staining. (A) Visualization of starch granules within *Arabidopsis* guard cells of intact leaves. Scale bar 15 µm. Starch levels in guard cells were quantified using pseudo-schiff propidium iodide starch staining, as described previously [17]. (B) Data are the mean of ± SEM of guard cell starch area (μm^2) per stomata. Unpaired Student's *t* test showed significantly higher quantities in guard cell starch levels of 800 p.p.m. exposed plants when compared to 100 p.p.m. exposed plants (**P = 1.6E-09, n = 38 (100 p.p.m.) and n = 43 (800 p.p.m.) stomata. Data obtained from three independent pools of leaves, leaves number 5 and 6, from three different plants, for each treatment.

Plant growth conditions

Arabidopsis thaliana seeds were germinated under sterile conditions on 1/2 strength MS medium [62] dissolved in 0.8% (w/v) agar, 0.8% (w/v) sucrose, and adjusted to pH 5.8 with 1 N KOH. Seeds were stratified for 2 days at 4 °C. Ten-day-old seedlings were transferred to soil (Sunshine Professional Blend or Klasmann-Deilmann substrate select special mixture) containing slow release Osmocote fertilizer (4 $g{\cdot}L^{-1}$) and watered every 3 days to avoid water stress. All plants were grown in controlled growth room or a Conviron growth chamber under uniform temperature of 15–19 °C during the night (dark period) to 21–26 °C during the day (light period), relative humidity (RH) of 60–85% humidity with a leaf-height photon flux density of ~ 100–150 $\mu mol{\cdot}m^{-2}{\cdot}s^{-1}$. Plants were growing under a short-day photoperiod (SD) of 8 h light/16 h dark cycle, a medium-day length photoperiod (MD) under a 12 h/12 h light cycle, or a long-day photoperiod (LD) under a 16 h light/8 h dark cycle. Plants were 5- to 7-week old when selected for gas exchange experiments. Only plants that had not bolted were used in gas exchange experiments.

Accession numbers

The *Arabidopsis* loci investigated in this study have the following accession numbers: At5g48300 (*ADG1*), AT1G10760 (*SEX1*), AT3G23920 (*BAM1*), AT4G17090 (*BAM3*).

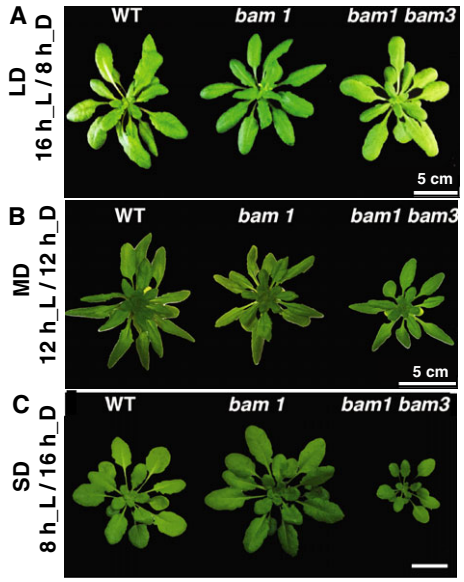

Fig. 2. β -amylase mutant plants. Photographs (A–C) of 6-week-old wild-type (WT), *bam1* and *bam1 bam3* double mutant plants grown under (A) long-day (LD, 16 h light/8 h dark cycle) and (B) medium-day (MD, 12 h light/12 h dark cycle) and (C) short-day length photoperiods (SD, 8 h light/16 h dark cycle).

Starch stain analyses

Qualitative starch staining was performed as previously described in Azoulay-Shemer *et al.* [47] on the 5th true leaf. In starch stain experiments that monitored starch levels in guard cell following exposure to high or low CO_2, a consistent atmospheric control chamber (COY, Michigan, USA) with additional top light (Agrolight, Beit Yehoshua, Israel) and a CO_2 sensor was used. The sealed chamber maintained light intensity 150 $\mu mol{\cdot}m^{-2}{\cdot}s^{-1}$, temperature of 21-23°C, and relative humidity of 58–62%. All the parameters were set and controlled automatically by ultra-sonic humidifier and chemical desiccant dried system together with heater and cooler system. Levels of 100 ppm CO_2 were maintained by mixing 'zero air' with atmospheric air; 800 ppm were maintained by mixing a CO_2 (5%) with atmospheric air. In addition, for quantitative guard cell starch analyses, leaf # 5 and #6 were collected 12 h after the start of the light period from wild-type (WT) and *adg1-1* plants grown under 12 h light/12 h dark or 16 h light/8 h dark (LD) light cycle ($n = 8$ plants, for each genotype). Two

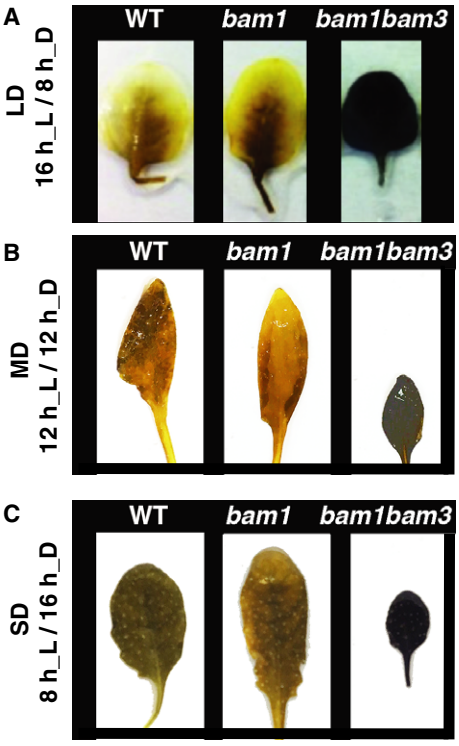

Fig. 3. Starch excess in β-amylase mutant plants. Starch staining in 5th true leaves of wild-type (WT), *bam1* and *bam1 bam3* double mutant plants grown under (A) long-day (LD, 16 h light/8 h dark cycle) and (B) medium-day (MD, 12 h light/12 h dark cycle) and (C) short-day length photoperiods (SD, 8 h light/16 h dark cycle). Mutant plants were harvested at the end of the night (A) or 1 h after the light period started (B, C). Plants were decolorized in hot 80% (v/v) ethanol and stained for starch with Lugol's solution. Experiments as shown in the figure were repeated at least three times.

leaves (# 5 and #6) from each plant were blended for 30 s in water. Epidermal peels were collected with a 200 μm mesh and immediately fixed in 50% (v/v) methanol, 10% (v/v) acetic acid at 4 °C for 12 h. Starch granules were stained with pseudo-schiff propidium iodide (PS-PI) and imaged as described in the detailed protocol of Horrer *et al*. [17]. Microscopy was performed confocal laser scanning microscope (LSM 710; Carl Zeiss, Jena, Germany and TCS SP8; Leica Geosystems, St. Gallen, Switzerland), using an excitation wavelength of 488 nm and emission of 610–640 nm. Starch granule area was measured using IMAGE J (NIH, http://rsbweb.nih.gov/ij/). The presented data are means ± SEM. Stomatal numbers are indicated in figure legends.

Gas exchange measurements

Gas exchange measurements were conducted on the 5th or 6th fully expanded true leaf, from intact mature rosettes of nonsenescent 5- to 7-week-old WT and mutant/transgenic plants. All measurements were carried out in the initial 1–4 h after the beginning of day (light on), using Li-6400, Li-6400XT, and Li6800 infrared (IR-GA) gas exchange analyzer systems with a fluorometer chambers (LI-COR Inc., Lincoln, NE, USA). Gas exchange analyzers were calibrated on each experimental day. The following conditions were held constant in the Licor measurement chamber: photon flux density of 150 $\mu mol \cdot m^{-2} \cdot s^{-1}$ (10% blue), temperature of 21 °C, and relative humidity of 59–61%. When the leaf area was smaller than chamber diameter, leaf area was measured and used in data analyses. In all experiments, wild-type and mutant plants were grown side by side, under the same growth conditions and analyzed in the same time period. Figures show data comparing WT and mutant responses collected within the same experimental sets as described previously [47].

Stomatal responses to [CO_2] shifts were investigated as follows: For stomatal opening experiments, stomatal conductance was stabilized at the indicated beginning [CO_2] (e.g., 360 p.p.m.) for 30 min. Next, [CO_2] was shifted to the indicated concentration of 800 p.p.m. then changed to the final CO_2 concentration of 100 p.p.m. as shown in the figures. The presented data show means ± SEM. For each genotype, data of 3–5 leaves (as indicated in figure legends)

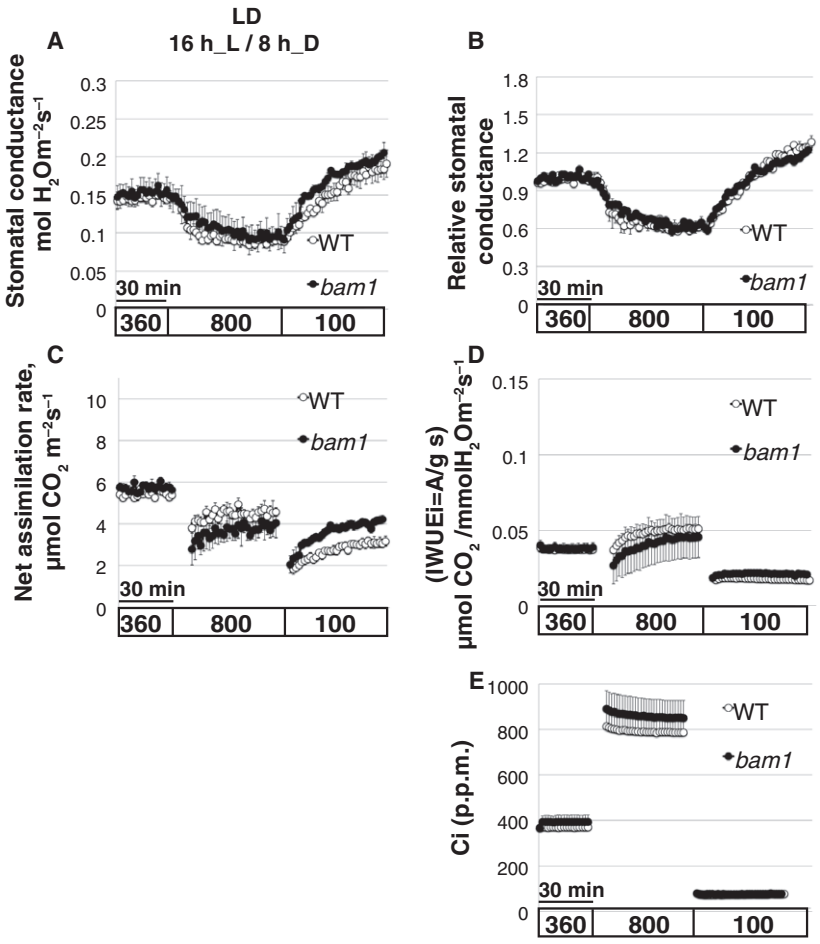

Fig. 4. The *Arabidopsis bam1* single mutant grown under long-day (16 h light/8 h dark) cycle shows normal wild-type-like stomatal response to CO_2 shifts. Time-resolved stomatal conductance responses and net carbon assimilation rates at the imposed [CO_2] shifts (bottom in p.p.m.) in wild-type (WT) and *bam1* mutant leaves. (A–D) Plants were analyzed using intact whole leaf gas exchange. (A) Stomatal conductance in mol H_2O $m^{-2}s^{-1}$. (B) Data shown in (A) were normalized to the stomatal conductance at 360 p.p.m. [CO_2] exposure before the change to 800 p.p.m. [CO_2]. (C) Shows net carbon assimilation rates ($\mu mol\ CO_2 \cdot m^{-2} \cdot s^{-1}$). (D) Shows intrinsic water use efficiency (iWUE) ($\mu mol\ CO_2/mmol\ H_2O \cdot m^{-2} \cdot s^{-1}$). (E) The corresponding intercellular [CO_2] (Ci) levels, calculated based on the stomatal conductance and ambient CO_2 concentration. Gas exchange data of WT plants are the same as those presented in Fig. 5, as data in Figs 4 and 5 were obtained within the same experimental datasets. Data in (A–E) are the mean of $n = 3$ leaves per genotype, with each leaf originating from different plants ± SEM.

were averaged. Each leaf was the 5th or 6th true leaf from a different plant. Relative stomatal conductance was calculated by normalization of each stomatal conductance to the stomatal conductance at the starting [CO_2] immediately prior to the transition to the second [CO_2]. [C_i] (μmol CO_2 mol·air^{-1}) was calculated using the Li-Cor analyzer, based on the model of Von Caemmerer and Farquhar [63] (see www.licor.com/env). As reported previously, absolute values of steady-state stomatal conductance values differed at different times of year [47] and therefore each experimental dataset was obtained with parallel-grown plants of the indicated genotypes. In addition, independent datasets were obtained showing the robustness of findings independent of the absolute stomatal conductance.

During the transition from 360 to 800 p.p.m. and from 800 to 100 p.p.m. [CO_2], net CO_2 assimilation rates, cannot be accurately calculated by the gas exchange analyzer, resulting in several minutes of noisy data. To ease data presentation and view the range of subsequent changes, ~ 3 min of the data points after each [CO_2] shift were removed in the following panels: net CO_2 assimilation, iWUE, and Ci.

Results

In a previous study, we found that mutant alleles in the AGPase starch biosynthesis enzyme, grown under MD (12 h light/12 h dark) photoperiod growth conditions, resulted in a reduced CO_2-induced stomatal closure response [47]. These results raise two critical questions: (a) Do starch degradation mutants (in addition to starch synthesis mutants) affect high CO_2-induced stomatal closing or low CO_2-induced stomatal opening responses? and (b) Do photoperiod growth conditions, affect stomatal conductance responses to CO_2? To determine whether shifts in [CO_2] affect guard cell starch levels, intact WT *Arabidopsis* plants, grown under SD conditions were exposed for 45 min to high or low CO_2, and their guard cell starch levels were quantified by starch pseudo-schiff stain confocal imaging [17]. The results clearly show significantly higher starch quantities in guard cells of plants exposed to 800 p.p.m. CO_2 when compared to those exposed to 100 p.p.m. CO_2 (Fig. 1). These data show that low CO_2, that mediates stomatal opening, is

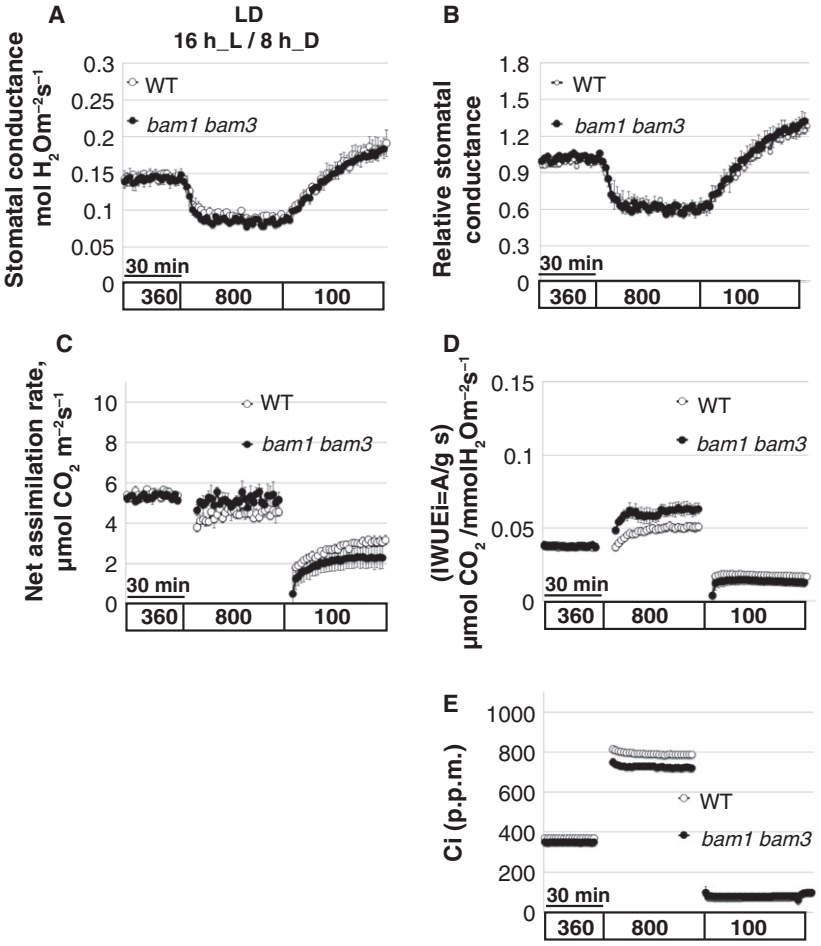

Fig. 5. The *Arabidopsis bam1 bam3* double mutant grown under long-day (16 h light/8 h dark) cycle shows normal wild-type-like stomatal response to CO_2 shifts. Time-resolved stomatal conductance responses and net carbon assimilation rates at the imposed [CO_2] shifts (bottom in p.p.m.) in wild-type (WT) and *bam1 bam3* mutant leaves. Plants were analyzed using intact whole leaf gas exchange. (A) Stomatal conductance in mol $H_2O{\cdot}m^{-2}{\cdot}s^{-1}$. (B) Data shown in (A) were normalized to the stomatal conductance at 360 p.p.m. [CO_2] exposure before the change to 800 p.p.m. [CO_2]. (C) Shows net carbon assimilation rates (μmol $CO_2{\cdot}m^{-2}{\cdot}s^{-1}$). (D) Shows intrinsic water use efficiency (iWUE) (μmol CO_2/mmol H_2O $m^{-2}s^{-1}$). (E) The corresponding intercellular [CO_2] (Ci) levels were calculated based on the stomatal conductance and ambient CO_2 concentration. Gas exchange data of WT plants are the same as those presented in Fig. 4, as data in Figs 4 and 5 were obtained within the same experimental datasets. Data in (A–E) are the mean of $n = 3$ leaves per genotype, with each leaf originating from different plants ± SEM for each genotype.

indeed accompanied by a reduction in starch levels in guard cells in *Arabidopsis*, consistent with previous studies in several plant species [3,33].

To determine whether well-known starch degradation mutants affect CO_2-induced stomatal movements, we investigated the β-amylase mutants, *BAM1* and *BAM3*, as these two genes are the most highly expressed plastid β-amylase genes in *Arabidopsis* leaves and have been shown to possess different cell-type-specific functions [17]. *BAM1* is highly expressed in guard cells in young nonflowering plants [64]. Also, *BAM1* RNAi and *bam1* mutant plants exhibit a guard cell-specific starch-excess phenotype [17], with no significant influence on mesophyll starch levels in nonflowering plants under standard, nonstressed, conditions [25]. In contrast, *BAM3* is highly expressed in the mesophyll [64], and was reported as the main isoform in leaf mesophyll starch metabolism [25]. *BAM3* transcript level is less abundant in guard cells [17]. Silencing of *BAM3* [26] and *bam3* mutant plants (EMS: CS92461) [61] have been shown to overaccumulate starch in the mesophyll, while *bam3* guard cell starch levels are similar to wild-type (WT) [17]. Furthermore, *bam1* but not *bam3* mutants showed an impaired light-induced stomatal opening when compared to WT plants, which correlates with their cell type preferential expression patterns [17]. Together these data led us to investigate the role of the guard cell starch degrading enzymes BAM1 and BAM3 in stomatal conductance regulation in response to elevated CO_2 and reduced CO_2.

Starch mobilization was previously suggested to be under the control of the circadian clock [65]. Detailed analysis by Lu *et al.* [66] revealed a tight regulation of *BAM3* expression by the circadian clock. To determine to which degree starch degradation in mesophyll and guard cells is involved in CO_2-induce stomatal movements, and whether photoperiods affect stomatal responses *via* the regulation of starch degradation, we performed gas exchange analyses on wild-type (Col-0), *bam1* (SALK_039895), and *bam1 bam3* (SALK_039895 × CS92461) double mutant plants, grown under long-day 16 h light/8 h dark (LD), medium-day length (12 h/12 h, MD), and short-day (8 h light/16 h dark, SD) photoperiodic conditions.

BAM mutant plants showed retarded growth under SD conditions (Fig. 2C), which was less severe as day length increased (Fig. 2A,B). To verify the previously

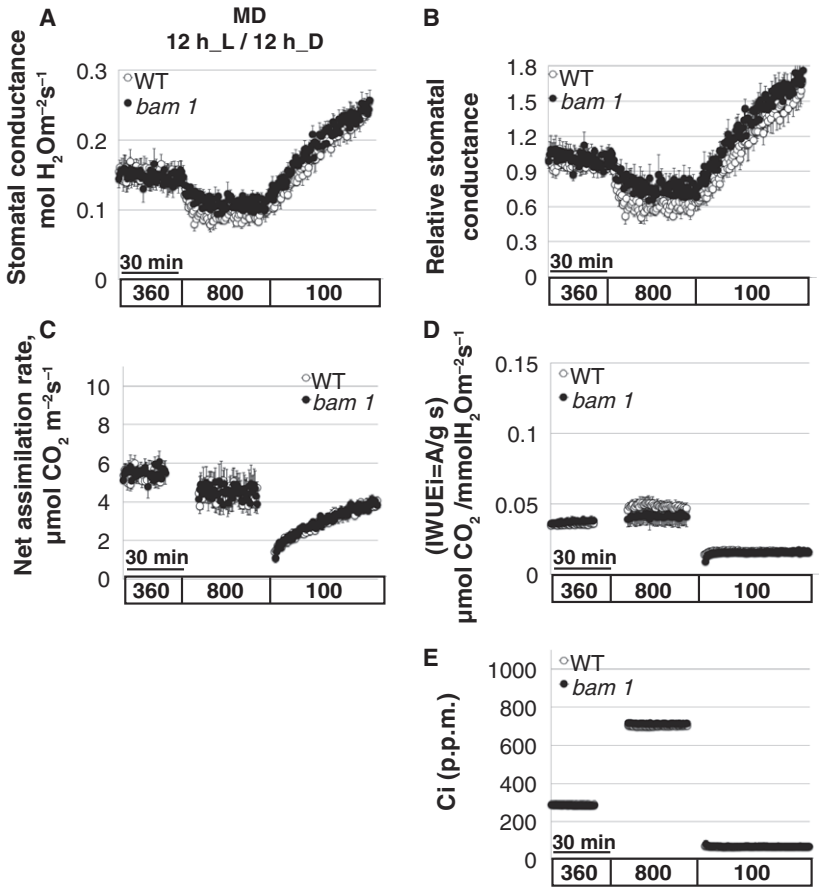

Fig. 6. The *Arabidopsis bam1* mutant grown under 12 h light/12 h dark (MD) cycle shows normal wild-type-like stomatal response to CO_2 shifts. Time-resolved stomatal conductance responses and net carbon assimilation rates at the imposed [CO_2] shifts (bottom in p.p.m.) in wild-type (WT) and *bam1* mutant leaves. Plants were analyzed using intact whole leaf gas exchange. (A) Stomatal conductance in mol $H_2O \cdot m^{-2} \cdot s^{-1}$. (B) Data shown in (A) were normalized to the stomatal conductance at 360 p.p.m. [CO_2] exposure before the change to 800 p.p.m. [CO_2]. (C) Shows net carbon assimilation rates (µmol $CO_2 \cdot m^{-2} \cdot s^{-1}$). (D) Shows intrinsic water use efficiency (iWUE) (µmol CO_2/mmol H_2O $m^{-2} s^{-1}$). (E) The corresponding intercellular [CO_2] (Ci) levels were calculated based on the stomatal conductance and ambient CO_2 concentration. Gas exchange data of WT plants are the same as those presented in Fig. 7, as data in Figs 6 and 7 were obtained within the same experimental datasets. Data in (A-E) are the mean of $n = 3$, with each leaf originating from different plants ± SEM for each genotype.

determined starch accumulation phenotypes in leaves of *bam1* and *bam1 bam3* double mutant plants [17,67], when grown under the imposed photoperiodic conditions (LD, MD, and SD), the 5th true leaves from Col-0 (WT), *bam1* and *bam1 bam3* were sampled at the end of the night (Fig. 3A,C), or 1 h after light was turned on (Fig. 3B) and stained with iodine as a measure of their starch content. The results under the imposed growth regimes confirmed a drastic overaccumulation of starch in rosette leaves of the *bam1 bam3* double mutant when compared to *bam1* and wild-type plants (Fig. 3A–C).

We next investigated stomatal conductance responses of both *bam1* and *bam1 bam3* mutant plants to CO_2 shifts in intact plants grown under LD (16 h light/8 h dark) (Figs 4 and 5), MD (12 h light/12 h dark) (Figs 6 and 7; Figs S1 and S2), and SD (8 h light/16 h dark) photoperiodic conditions (Fig. 8). Unexpectedly under all growth conditions, no dramatic differences were observed between *bam* mutants and WT stomatal conductance responses to CO_2 shifts (Fig. 4–8). In one experimental dataset, when shifting the CO_2 concentration from 400 to 100 p.p.m., we observed a slight nonsignificant enhanced stomatal opening response of *bam1* and *bam1 bam3* mutant compare to WT plant, when plants were grown under MD conditions (Figs S1 and S2 panels A and B, $P = 0.4$, unpaired Student's t test at the end of 100 p.p.m. [CO_2] step), which was not observed under LD growth conditions (Fig. S2 panels C and D). Net CO_2 assimilation rates were found to be similar to parallel-grown WT controls in *bam1* under all growth conditions (Figs 4C, 6C and 8C). However, *bam1 bam3* double mutant leaves showed reduced net CO_2 assimilation rates under high CO_2 levels, when plants grew under MD (Fig. 7C), but not under LD conditions (Fig. 5C). The derived intercellular CO_2 concentrations and calculated intrinsic water use efficiency data for all leaves are shown in Figs 4–8, panels D and E.

Next, we analyzed the *starch excess1* (*sex1*) mutant that is defective in the R1 regulator of starch degradation [12] (Figs 9–11, Fig. S3). As reported previously, the *sex1* mutant exhibits a dramatic overaccumulation of starch in *Arabidopsis* leaves (Fig. 10A and [12]).

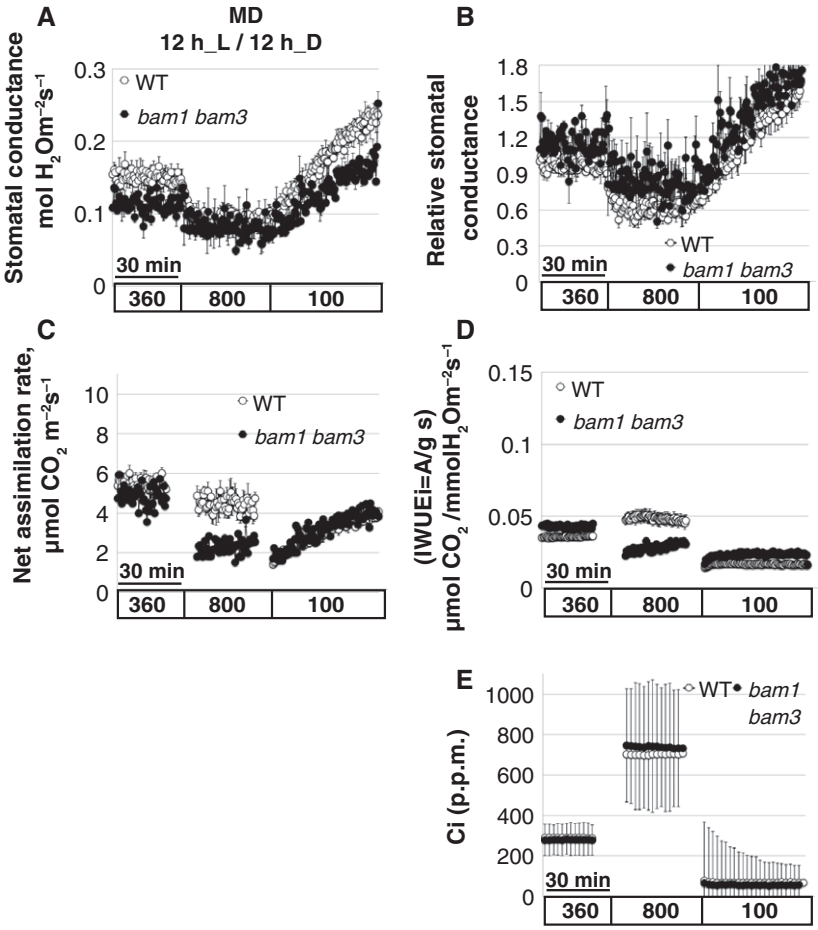

Fig. 7. The *Arabidopsis bam1 bam3* double mutant grown under 12 h light/12 h dark (MD) cycle shows normal wild-type-like stomatal response to CO_2 shifts, and reduced net CO_2 assimilation under high CO_2. Time-resolved stomatal conductance responses and net carbon assimilation rates at the imposed [CO_2] shifts (bottom in p.p.m.) in wild-type (WT) and *bam1 bam3* mutant leaves. Plants were analyzed using intact whole leaf gas exchange. (A) Stomatal conductance in mol $H_2O \cdot m^{-2} \cdot s^{-1}$. (B) Data shown in (A) were normalized to the stomatal conductance at 360 p.p.m. [CO_2] exposure before the change to 800 p.p.m. [CO_2]. (C) Shows net carbon assimilation rates (µmol $CO_2 \cdot m^{-2} \cdot s^{-1}$). (D) Shows intrinsic water use efficiency (iWUE) (µmol CO_2/mmol H_2O $m^{-2}s^{-1}$). (E) The corresponding intercellular [CO_2] (Ci) levels were calculated based on the stomatal conductance and ambient CO_2 concentration. Gas exchange data of WT plants are the same as those presented in Fig. 6, as data in Figs 6 and 7 were obtained within the same experimental datasets. Data in (A–E) are the mean of $n = 3$ leaves per genotype, with each leaf originating from different plants ± SEM for each genotype.

Data from plants grown under LD and MD conditions show that CO_2-regulated stomatal conductance responses in the *sex1-1* mutant were not dramatically different from wild-type leaves (Figs 9A,B and 10B,C). Notably, similar to the slight but statistically non-significant enhancement in average stomatal opening response observed in the starch degradation mutants *bam1* and *bam1 bam3* (Figs S1 and S2 panels A and B; MD growth conditions), when shifting the CO_2 concentration from 400 to 100 p.p.m., *sex1* mutant leaves showed a small but insignificant enhanced stomatal opening response, when plants were grown under LD conditions (Fig. S3, $P = 0.5$, unpaired Student's t test at the end of 100 p.p.m. [CO_2] step).

No major differences were observed in CO_2 assimilation rates and intrinsic water use efficiency of *sex1-1* plants compared to wild-type plants under the imposed CO_2 conditions (Figs 9C,D and 10D,E). Under SD conditions, *sex1-1* mutant showed a slightly reduced steady-state stomatal conductance (Fig. 11A). However, normalization of the data showed similar stomatal conductance responses in *sex1-1* and WT leaves (Fig. 11B). CO_2 assimilation rates were slightly reduced at high (800 p.p.m.) CO_2 levels (Fig. 11C). In sum unexpectedly, these analyses of the starch degradation mutants, *bam1 bam3* and *sex1* that overaccumulate starch in mesophyll and guard cells, as well as *bam1,* which accumulates starch solely in guard cells, revealed that there were no dramatic differences in rapid stomatal conductance responses to CO_2 changes under the imposed conditions and that stomata in intact leaves attached to intact soil-grown plants showed robust stomatal opening (Figs 4–11) despite a clearly reduced starch degradation in guard cells of these mutants.

In a previous study, we found that mutant alleles in the starch biosynthesis AGPase enzyme showed a reduced stomatal closing response to CO_2 elevation [47]. However, it remained unknown whether this *AGPase* mutant phenotype is linked directly to starch levels or to an intermediate metabolite that is affected in *AGPase* mutant alleles [47]. Given that previous

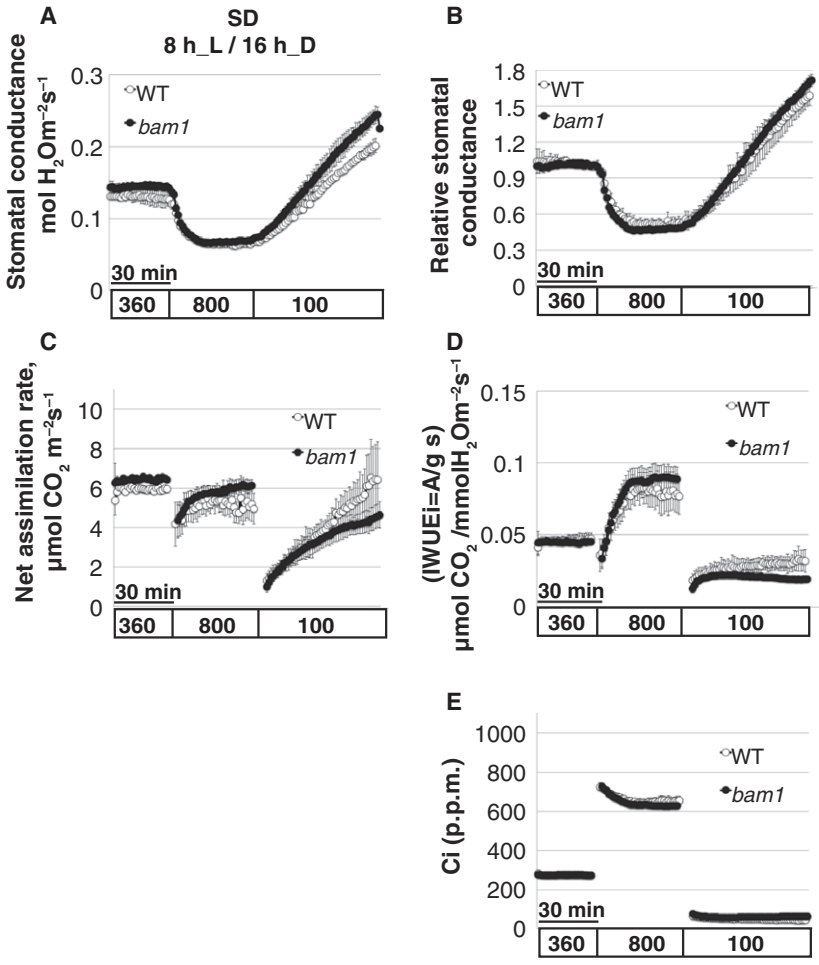

Fig. 8. The *Arabidopsis bam1* single mutant, grown under short-day (SD: 8 h light/16 h dark), shows wild-type-like stomatal responses to CO_2 shifts. Time-resolved stomatal conductance responses and net carbon assimilation rates at the imposed [CO_2] shifts (bottom in p.p.m.) in wild-type (WT) and *bam1* mutant leaves. Plants were analyzed using intact whole leaf gas exchange. (A) Stomatal conductance in mol $H_2O{\cdot}m^{-2}{\cdot}s^{-1}$. (B) Data shown in (A) were normalized to the stomatal conductance at 360 p.p.m. [CO_2] exposure before the change to 800 p.p.m. [CO_2]. (C) Shows net carbon assimilation rates (µmol $CO_2{\cdot}m^{-2}{\cdot}s^{-1}$). (D) Shows intrinsic water use efficiency (iWUE) (µmol CO_2/mmol H_2O $m^{-2}s^{-1}$). (E) The corresponding intercellular [CO_2] (Ci) levels were calculated based on the stomatal conductance and ambient CO_2 concentration. Data in (A–E) are the mean of $n = 3$ leaves per genotype, with each leaf originating from different plants ± SEM for each genotype.

experiments with the *AGPase* alleles were conducted under MD 12 h light/12 h dark photoperiodic conditions, and following the hypothesis that stomatal conductance may be dependent on day length *via* starch biosynthesis, we explored the CO_2 response of *AGPase* mutant alleles under additional light growth regimes. We investigated the CO_2 responses of *adg1-1* mutant alleles [9,48] grown under a long-day photoperiod with 16 h light and 8 h dark (LD). Interestingly, we observed that the CO_2-triggered reduction in stomatal conductance was similar in *adg1-1* and wild-type (Col-0) plants under LD conditions (Fig. 12A,B). As this differed from the CO_2 response in *AGPase* alleles under MD conditions [47], we tested *AGPase* mutant plants under shorter photoperiodic conditions. When plants were grown under SD (8 h light/16 h dark), we observed impairment in high CO_2-triggered reduction in stomatal conductance (Fig. 12C,D). CO_2 regulation of stomatal closing was clearly impaired in *adg1-1* mutants under SD (Fig. 12C,D) and MD conditions [47] compared to WT plants, but not under LD conditions (Fig. 12A,B).

To further test the impaired stomatal conductance responses to CO_2, observed under SD photoperiodic conditions (Fig. 12C,D), we investigated an independent *AGPase* mutant allele, *aps1* [9,48,49]. Consistent with the *adg1-1* allele, *aps1* leaves showed intact CO_2-induced stomatal closure when plants were grown under LD photoperiod (Fig. 13A,B), and a reduced stomatal response to high CO_2 under SD (Fig. 13C,D) growth conditions. Furthermore, under both photoperiod conditions (LD, SD), *AGPase* mutant plants showed intact low CO_2-induced stomatal opening (Figs 12 and 13 panels A and B & Fig. S8) and reduced photosynthetic rates at high (800 p.p.m.) CO_2 levels (Figs S4 panel A to S7 panel A).

A closer examination of Figs 12 and 13 and direct comparison of the stomatal conductance CO_2 response data of the two *AGPase* mutant alleles (*adg1-1*, *aps1*) showed no clear differences between LD- and SD-grown mutant plants (Fig. 14A,B; Gas exchange data of *adg1-1* and *aps1* plants were extracted from experiments in Figs 12 and 13, respectively). We therefore compared stomatal conductance responses of WT

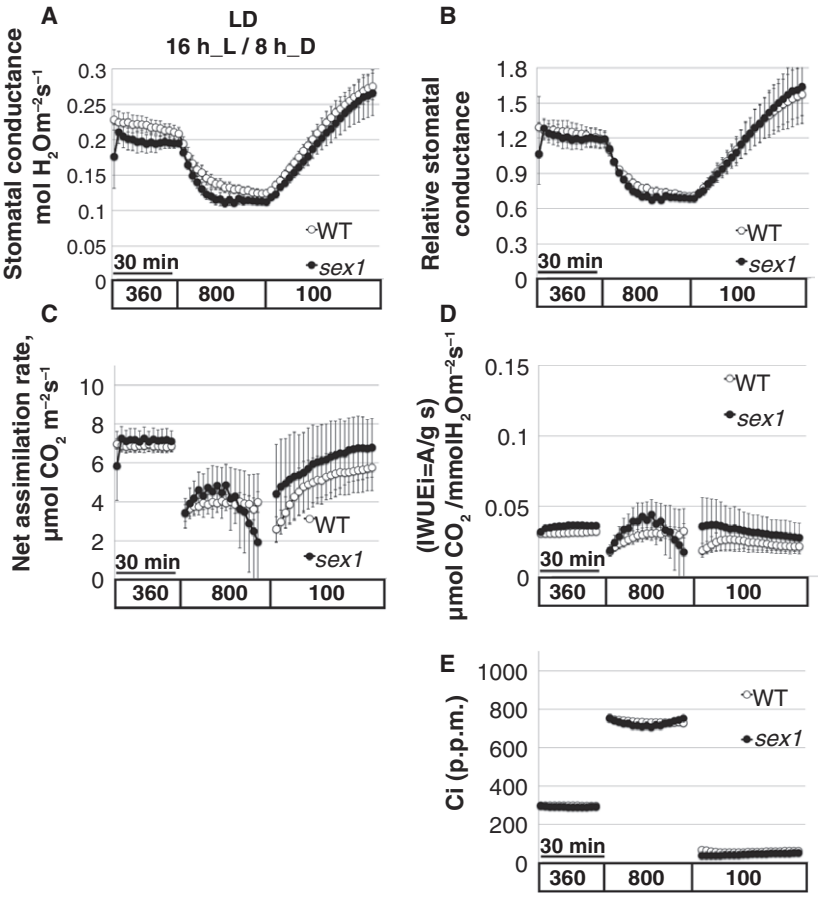

Fig. 9. The *Arabidopsis* starch overaccumulation *sex1-1* mutant, grown under long-day (16 h light/8 h dark) cycle shows normal wild-type-like stomatal responses to CO_2 shifts. Time-resolved stomatal conductance responses and net carbon assimilation rates at the imposed [CO_2] shifts (bottom in p.p.m.) in wild-type (WT) and *sex1-1* mutant leaves. Plants were analyzed using intact whole leaf gas exchange. (A) Stomatal conductance in mol $H_2O{\cdot}m^{-2}{\cdot}s^{-1}$. (B) Data shown in (A) were normalized to the stomatal conductance at 360 p.p.m. [CO_2] before the change to 800 p.p.m. [CO_2]. (C) Shows net carbon assimilation rates (µmol $CO_2{\cdot}m^{-2}{\cdot}s^{-1}$). (D) Shows intrinsic water use efficiency (iWUE) (µmol CO_2/mmol H_2O $m^{-2}s^{-1}$). (E) The corresponding intercellular [CO_2] (Ci) levels were calculated based on the stomatal conductance and ambient CO_2 concentration. Data in (A–E) are the mean of $n = 5$ (WT), $n = 3$ (*sex1-1*) leaves, with each leaf originating from different plants ± SEM for each genotype.

Arabidopsis plants, grown under LD and SD conditions, by extracting WT gas exchange data from experiments in Figs 9, 11–13 and additional experiments. The data clearly show that in response to high CO_2 WT plants grown under SD conditions reduce their stomatal conductance significantly more than plants grown under LD conditions (Fig. 15A,B, $P = 0.03$, unpaired Student's t test at the end of 800 p.p.m. [CO_2] step). Under ambient CO_2 levels, intrinsic water use efficiency (iWUE) was significantly higher in SD compared to LD-grown WT plants ($P = 0.04$, unpaired Student's t test at the end of 360 p.p.m. [CO_2] step), which further increased under high [CO_2] (Fig. 15D $P = 0.04$, at the end of 800 p.p.m. [CO_2] step).

We next investigated whether *AGPase* mutant plants show the well-known guard cell starch deficiency phenotype [47], under MD and LD photoperiodic growth conditions. Under both light regimes, the *adg1-1* mutant showed severe starch deficiency, in guard cells (Fig. S9, $n = 8$ plants for each genotype and growth condition, 25–30 images analyzed per genotype and

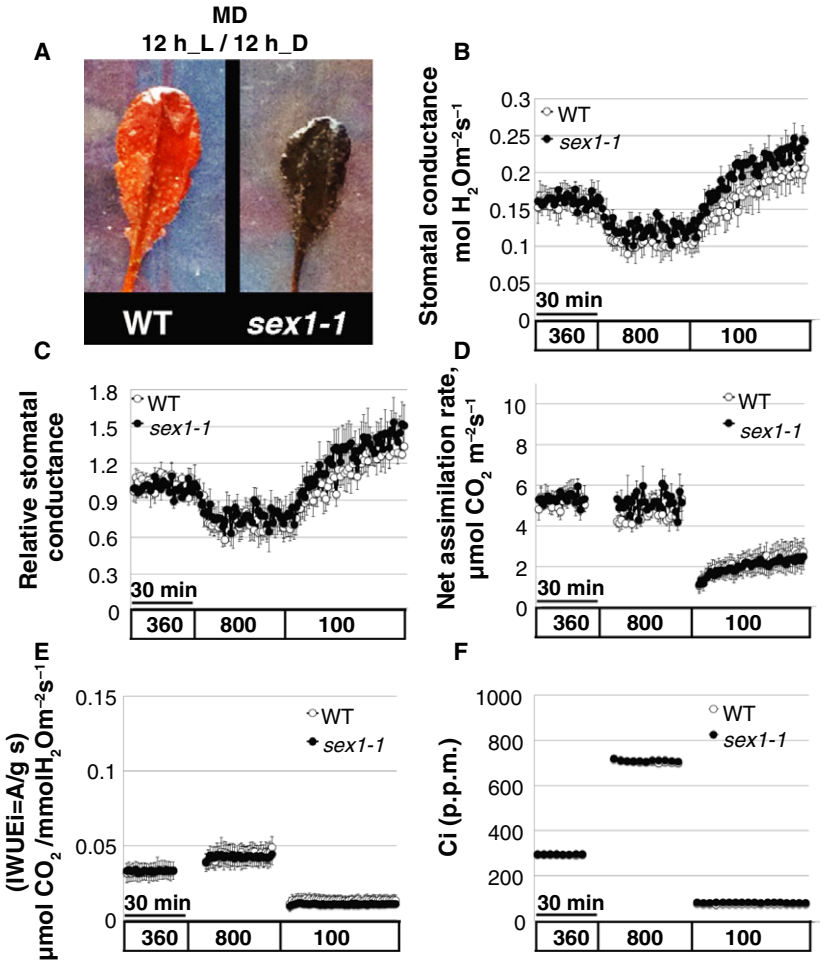

Fig. 10. The *Arabidopsis* starch overaccumulation *sex1-1* mutant, grown under 12 h light/12 h dark (MD) cycle, shows normal stomatal responses to CO_2 shifts. (A) Starch overaccumulation phenotype of the *sex1-1* mutant. Starch content in the 4th true leaf of 5-week-old wild-type (WT) and *sex1-1* mutant plants harvested at the end of the night. Plants were decolorized in hot 80% (v/v) ethanol and stained for starch with Lugol's solution. (B–F) Time-resolved stomatal conductance responses and net carbon assimilation rates at the imposed [CO_2] shifts (bottom in p.p.m.) in wild-type (WT) and *sex1-1* mutant. Plants were analyzed using intact whole leaf gas exchange. (B) Stomatal conductance in mol $H_2O \cdot m^{-2} \cdot s^{-1}$. (C) Data shown in (B) were normalized to the stomatal conductance of 360 p.p.m. [CO_2] exposure before the change to 800 p.p.m. [CO_2]. (D) Shows net carbon assimilation rates (µmol $CO_2 \cdot m^{-2} \cdot s^{-1}$). (E) Shows intrinsic water use efficiency (iWUE) (µmol CO_2/mmol H_2O $m^{-2}s^{-1}$) for each genotype. (F) The corresponding intercellular [CO_2] (Ci) levels, calculated based on the stomatal conductance and ambient CO_2 concentration. Data in (B–F) are the mean of wild-type $n = 4$, and *sex1-1* $n = 3$ leaves, with each leaf originating from different plants ± SEM for each genotype.

condition), consistent with previous studies showing a strong starch deficiency phenotype in *aps1* for LD [68,69], in *aps1* and *adg1-1* for LD [49] and in *adg1-1* and *aps1* for MD (12 h/12 h) photoperiods [9,47,50].

Discussion

Mutants in starch degradation enzymes BAM1, BAM3, and SEX1 did not dramatically impair CO_2-regulated stomatal movements

The model, in which starch metabolism regulates stomatal opening and closure, suggests that signals that induce stomatal opening will stimulate starch degradation. Based on this model, reduced starch degradation in guard cells would be expected to result in an impaired stomatal opening. SEX1 and BAM3 are key enzymes that mediate nighttime starch degradation [12,26], while BAM1 functions in guard cell starch degradation in response to light [17]. In the present study, analysis of *sex1, bam1*, and *bam1 bam3* double mutant plants showed largely intact stomatal conductance responses to CO_2 shifts (Figs 4–11). The present study suggests that the key starch degradation enzymes, BAM1, BAM3, and SEX1, are not rate-limiting for CO_2-regulated stomatal movements. BAM1 is the major plastidic β-amylase in guard cells, and its role in guard cell starch degradation and stomatal movements in response to blue light and drought was previously demonstrated [17,70]. Distinct mechanisms mediating starch degradation in different tissues have been discussed [71], and other debranching enzymes may be involved in CO_2-induced starch degradation. BAM1, AMY3, LDA, and ISA3 could function together in guard cell starch mobilization during stomatal opening [17], and redundancy in their starch degradation activity may need further investigation by generation and analyses of higher order mutants. For example, *amy3* (α--*amylase* 3) *bam1* double mutant plants show impaired phototropin-dependent light-induced stomatal opening together with impaired starch degradation in guard cells [17] and the *amy3 bam1* double mutant combination may result in a rate-limiting response to low CO_2. In addition, studies have suggested other sources for osmolytes that contribute to stomatal opening. Malate and sucrose are imported

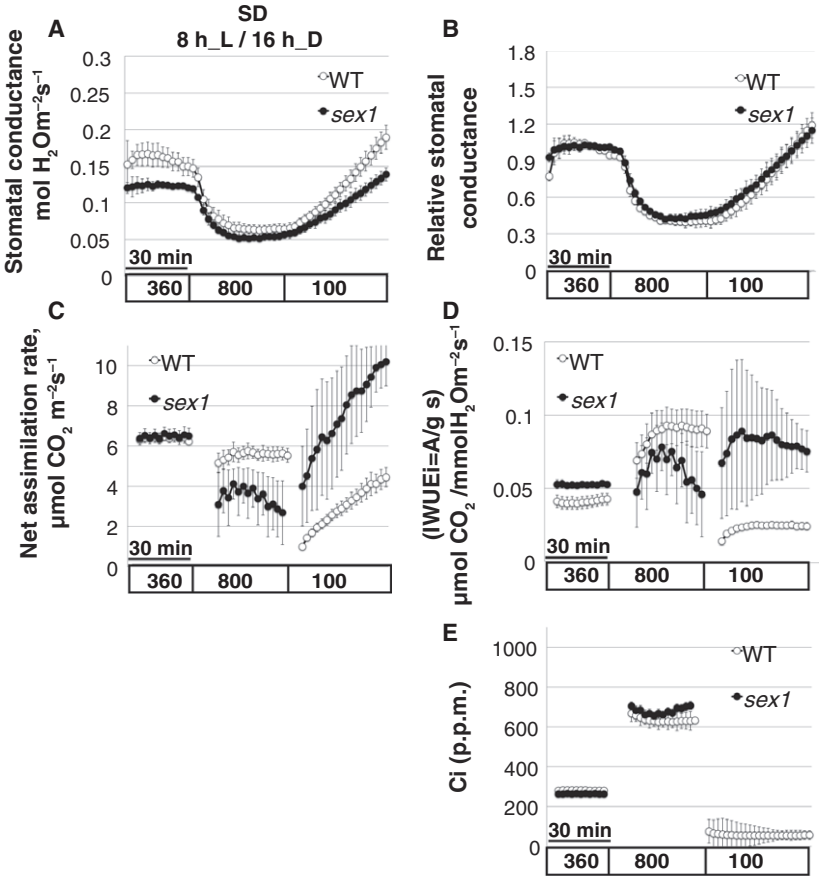

Fig. 11. Stomatal response to CO_2 shifts of the *Arabidopsis* starch overaccumulation *sex1-1* mutant, grown under short-day (8 h light/16 h dark) cycle. Time-resolved stomatal conductance responses and net carbon assimilation rates at the imposed [CO_2] shifts (bottom in p.p.m.) in wild-type (WT) and *bam1 bam3* mutant leaves. Plants were analyzed using intact whole leaf gas exchange. (A) Stomatal conductance in mol $H_2O{\cdot}m^{-2}{\cdot}s^{-1}$. (B) Data shown in (A) were normalized to the stomatal conductance at 360 p.p.m. [CO_2] exposure before the change to 800 p.p.m. [CO_2]. (C) Shows net carbon assimilation rates (µmol $CO_2{\cdot}m^{-2}{\cdot}s^{-1}$). (D) Shows intrinsic water use efficiency (iWUE) (µmol CO_2/mmol H_2O $m^{-2}s^{-1}$). (E) The corresponding intercellular [CO_2] (Ci) levels were calculated based on the stomatal conductance and ambient CO_2 concentration. Data in (A–E) are the mean of $n = 4$ (WT), $n = 3$ (*sex1-1*) leaves, with each leaf originating from different plants ± SEM for each genotype.

from the mesophyll to the guard cells and were previously suggested to be involved in stomatal conductance regulation [43,72].

Poffenroth *et al.* [32] showed that only blue light, but not red light, induces guard cell starch degradation and sugar accumulation during stomatal opening, in *Vicia faba*. Similarly, only nonphotosynthetic blue light has been reported to induce increases in K^+ content and guard cell starch degradation during stomatal opening, while exposure to red light or photosynthetic (high intensity) blue light did not alter K^+ and starch content in guard cells [21]. These findings are consistent with the model that guard cells can produce other osmolytes including sugars during stomatal opening. Note that chloride ions may also replace malate under conditions that preclude malate synthesis [19,20].

The present study provides evidence that during low CO_2-induced stomatal opening, the key starch-degrading enzymes, BAM1, BAM3, and SEX1, do not play a pivotal role in providing osmolytes for stomatal opening. Future metabolic investigation of starch metabolic mutants is needed to determine whether starch independent osmolytes including chloride, nitrate, and sucrose uptake play predominant roles in this response.

Stomatal conductance responses to CO_2 shifts are not directly dependent on starch level

Outlaw and Manchester [3] demonstrated the negative correlation of starch levels and stomatal aperture. Since then, many studies have shown the relevance of starch metabolism to stomatal aperture regulation [3,16,17,21,32,33,47,64,70]. Here we unexpectedly find that kinetic stomatal conductance responses to [CO_2], in starch-excess and starchless mutants do not strictly correlate with steady-state starch levels in leaves or in guard cells. We observed wild-type CO_2-induced stomatal conductance responses in the starch overaccumulation mutants *bam1 bam3* (Figs 5A and 7A) and *sex1-1* (Fig. 9B). Furthermore, the guard cell starch-excess mutant *bam1* showed full stomatal closure and largely intact stomatal opening responses to CO_2 shifts comparable to wild-type leaves, under all three photoperiod growth conditions (Figs 4A, 6A and 8A,

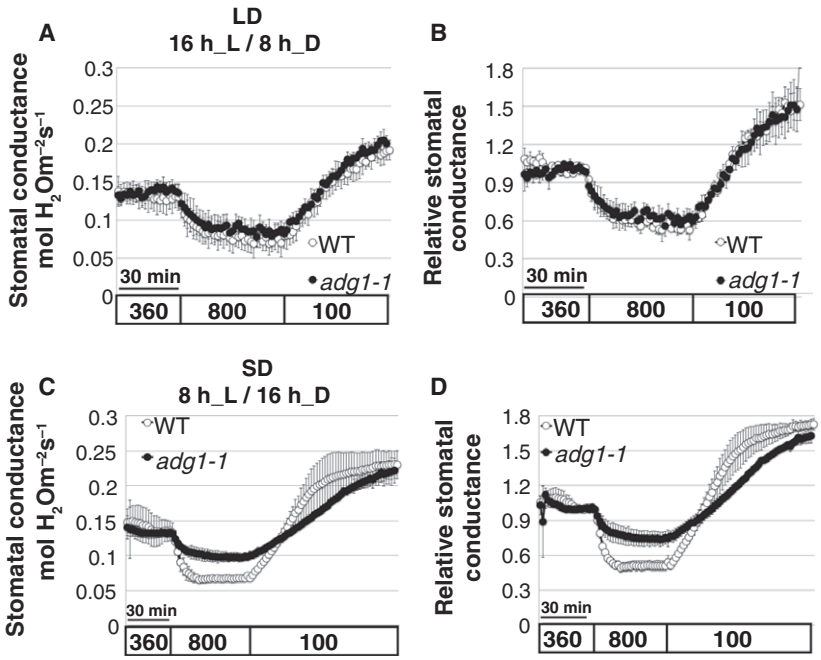

Fig. 12. The *Arabidopsis* starch degradation mutant *adg1-1* shows an impaired stomatal response to CO_2 shifts compared to WT, when plants were grown under short-day (SD: 8 h light/16 h dark) but not when grown under long-day (LD; 16 h light/8 h dark) cycle. Time-resolved stomatal conductance responses at the imposed [CO_2] shifts (bottom in p.p.m.) in wild-type (WT) and *adg1-1* mutant. (A-D) Plants were analyzed using intact whole leaf gas exchange. (A, C) Stomatal conductance in mol $H_2O \cdot m^{-2} \cdot s^{-1}$. (B, D) Data shown in (A and C) were normalized to the stomatal conductance of 360 p.p.m. [CO_2] exposure before the change to 800 p.p.m. [CO_2]. Data in (A–D) are the mean of $n = 4$ leaves, with each leaf originating from different plants ± SEM for each genotype. NOTE: Stomatal conductance responses to CO_2 change in WT and *adg1-1* plants grown under 12 h light/12 h dark (MD) conditions were published on [47]. For the corresponding assimilation rates, iWUE and Ci data from these experiments see Figs S4 and S5.

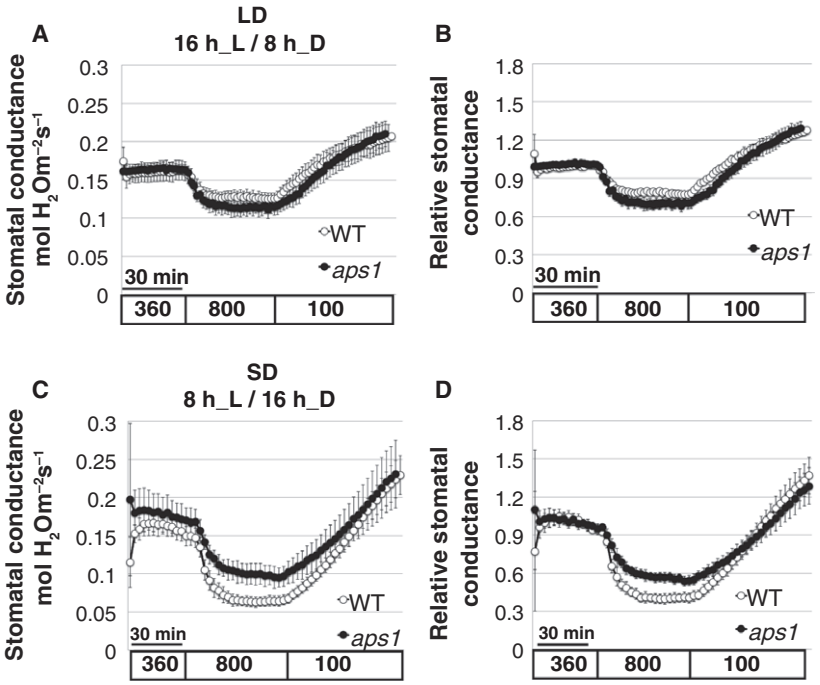

Fig. 13. The *Arabidopsis* starch degradation mutant *aps1* shows an impaired stomatal response to CO_2 shifts, when plants were grown under short-day (SD: 8 h light/16 h dark) but not when plants were grown under long-day (LD; 16 h light/8 h dark) cycle. Time-resolved stomatal conductance responses at the imposed [CO_2] shifts (bottom in p.p.m.) in wild-type (WT) and *aps1* mutant. (A-D) Plants were analyzed using intact whole leaf gas exchange. (A, C) Stomatal conductance in mol $H_2O \cdot m^{-2} \cdot s^{-1}$. (B, D) Data shown in (A, C) were normalized to the stomatal conductance of 360 p.p.m. [CO_2] exposure before the change to 800 p.p.m. [CO_2]. Data are the mean of $n = 4$ (A, B) and $n = 3$ (C, D) leaves, with each leaf originating from different plants ± SEM for each genotype. For the corresponding CO_2 assimilation rates, iWUE and Ci data see Figs S6 and S7.

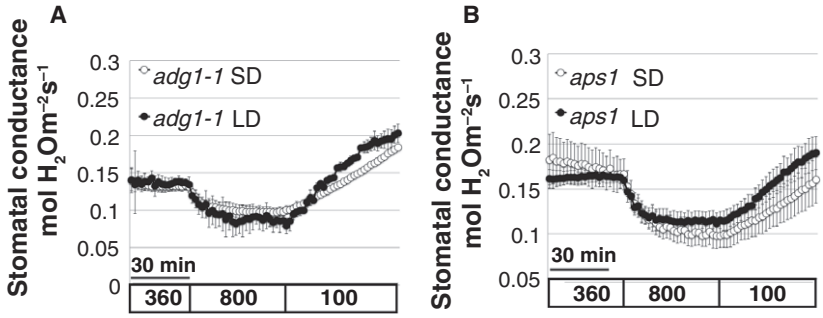

Fig. 14. Stomatal conductance responses to CO_2 shifts of *AGPase* mutant plants, grown under short-day (SD: 8 h light/16 h dark) and long-day (LD; 16 h light/8 h dark) cycle, are not significantly different. Time-resolved stomatal conductance responses at the imposed [CO_2] shifts (bottom in p.p.m.) in *AGPase* mutant (*adg1-1, aps1*) grown under SD or LD cycle. Plants were analyzed using intact whole leaf gas exchange. (A, B) Stomatal conductance in mol $H_2O \cdot m^{-2} \cdot s^{-1}$. Gas exchange data of *adg1-1* and *aps1* plants were extracted from experiments in Figs 11 and 12, respectively.

Fig. S1). In addition, starch biosynthesis *AGPase* mutant alleles showed wild-type-like CO_2-induced stomatal conductance responses under long-day photoperiod (Figs 12A and 13A), and an impaired response under 12 h/12 h photoperiod [47] and short-day photoperiod compared to WT plants (Figs 12C,D and 13C,D). However, *adg1-1* guard cell starch levels were dramatically reduced under both growth conditions (Fig. S9), as was previously documented for *adg1-1* and *aps1* alleles grown under MD and LD [9,47,49,50].

Photoperiod effects on CO_2-regulated stomatal conductance responses in WT and guard cell starch metabolism mutants

In a previous study, *AGPase* mutant plants grown under a MD (12 h light/12 h dark) photoperiod showed impaired stomatal closure in response to high CO_2 compared to WT controls [47]. Here we show that this impaired response is restricted to plants that were grown under MD or SD, but not LD photoperiod. Together, these data imply an effect of day

length on high CO_2-induced stomatal closure *via* guard cell starch metabolism.

Stomatal movements were recently proposed to depend on interactions between light signals and rhythmic starch turnover [73]. Starch synthesis rates are larger during short-days compared to long-day photoperiods [66,74]. The key regulatory starch biosynthesis enzyme AGPase was previously shown to be controlled by the circadian clock. The *Chlamydomonas* AGPase displays circadian oscillations in its protein and activity levels [75]. A circadian oscillation pattern was also detected for the *AGPase* mRNA in *Arabidopsis* [65]. Two detailed studies, by Gibon *et al.* [74] and Mugford *et al.* [76], which have analyzed the regulatory properties of AGPase under different photoperiods, revealed an increase in post-translation activation of AGPase when day length was reduced to SD (8 h light/16 dark) growth conditions. Together these studies support a model in which the increased AGPase activity in SD-grown WT plants would enhance CO_2-induced stomatal closing compared to LD-grown WT plants, consistent with results from the present study (Fig. 15). These data are consistent with the model that mutant alleles in the *AGPase* gene would be predicted to show a reduced stomatal response to elevated CO_2 compared to wild-type plants, when plants are grown under SD conditions, as found in the present study. As stomatal closing includes synthesis of the osmotically inactive starch, the enhanced stomatal closing in SD-grown wild-type

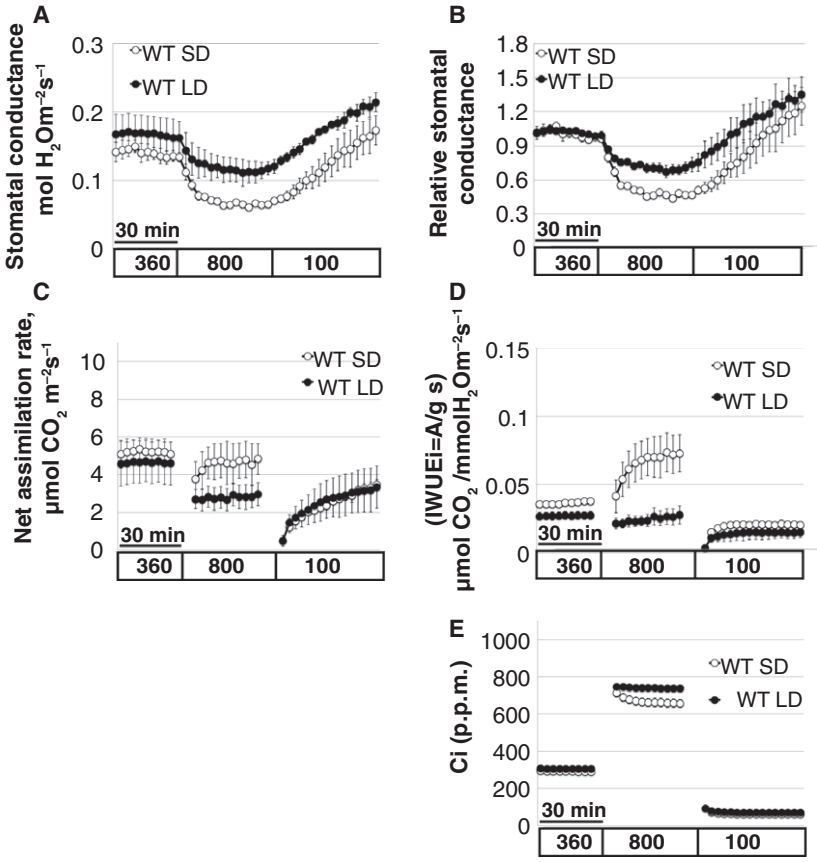

Fig. 15. Stomatal response to CO_2 elevation of WT *Arabidopsis* plants grown under (SD: 8 h light/16 h dark) is significantly more pronounced than of WT plants grown under long-day (LD; 16 h light/8 h dark) cycle. Time-resolved stomatal conductance responses at the imposed [CO_2] shifts (bottom in p.p.m.) in wild-type (WT) grown under SD or LD cycle. (A-E) Plants were analyzed using intact whole leaf gas exchange. (A) Stomatal conductance in mol $H_2O \cdot m^{-2} \cdot s^{-1}$. (B) Data shown in (A) were normalized to the stomatal conductance at 360 p.p.m. [CO_2]. Gas exchange data of WT plants were extracted from several experiments, including data shown in Figs 9, 11–13. Data are the mean of $n = 3$ experiments, for each growth condition (in each experiment data from three to four leaves were averaged, with each leaf originating from a different plant). Unpaired Student's *t* test investigating statistical significance between SD- and LD-grown WT plants showed a significantly lower stomatal conductance under high [CO_2] ($P = 0.03$, at the end of the 800 p.p.m. [CO_2] step) and significantly larger intrinsic water use efficiencies under ambient CO_2 ($P = 0.04$, at the end of 360 p.p.m. [CO_2] step) and high CO_2 ($P = 0.04$, at the end of 800 p.p.m. [CO_2] step).

plants vs. LD-grown wild-type plants was not observed in the two *AGPase* mutant alleles (Fig. 14), but was observed in wild-type plants (Fig. 15). These data point to a model in which starch synthesis in guard cells becomes rate-limiting for high CO_2-induced stomatal closing in SD-grown plants, due to the increased AGPase activity under these growth conditions. Future research will be required to test this model. At the end of the night (12 h dark and longer nights), sugar depletion inhibits carbohydrate utilization, which leads to a temporary buildup of sugar after the light period starts. High sugar levels are known to enhance the activation of AGPase by a post-translational redox regulation mechanism [77–79] and by allosteric activation [76], and by transcriptional regulation [80]. Indeed, the burst increase in sugar at the beginning of the day was found to be higher and more pronounced under short day than long day [57], resulting in an increase in the post-translational activation of AGPase activity [74] and resulted in partitioning of a larger proportion of the photoassimilate to starch [81,82]. Together, these observations may explain the rate-limiting role of AGPase in stomatal closure under short-day but not long-day photoperiod. Under short days, AGPase would have a larger role in photoassimilate partitioning into starch biosynthesis, and therefore might also affect the concentration of metabolites that function in CO_2 control of stomatal movements. Future in depth, guard cell metabolite analyses of starch metabolism mutants, grown under LD and SD conditions, could lead to further insights into the underlying mechanisms.

Unexpectedly, the present study shows that mutations in the starch degradation genes *BAM1, BAM3*, and *SEX1* did not significantly affect the kinetics and magnitude of low CO_2-induced stomatal opening. These findings point to possible models for future analyses that either (a) the key starch degradation enzymes, BAM1, BAM3, and SEX1, are not directly involved in low CO_2-triggered signal transduction that mediates stomatal opening; (b) a degree of starch degradation occurs *via* alternate or overlapping genes or pathways that are not completely abolished in guard cells of *sex1, bam1*, or *bam1 bam3* mutants, and are sufficient to provide guard cells with adequate amounts of organic osmolytes including the counter ion malate for intact stomatal opening; or (c) that starch degradation has only a minor, rate-limiting, effect on stomatal opening under the imposed conditions in soil-grown *A. thaliana* plants. Future research will be required to distinguish these or other models. Furthermore, future metabolic analyses of guard cells in the investigated mutants and under the range of investigated photoperiods could shed light on key metabolites that function in CO_2 regulation of stomatal movements.

Interestingly, net CO_2 assimilation rates were significantly reduced in both alleles of the starch biosynthesis mutant, *adg1-1* and *aps1* following a shift to high [CO_2], when compared to WT levels (Figs S4–S7). Similar significant reductions were observed, in leaves of the starch degradation *bam1 bam3* (Fig. 7C) and *sex1* mutants (Fig. 11C). These mutants accumulate starch in mesophyll cells (Figs 3 and 10) (*bam3* [25,61], *sex1* [12]). This behavior has been associated with a limitation of export of carbon from the Calvin–Benson cycle, the regeneration of Pi for photophosphorylation, and ultimately RuBP regeneration [83,84] which was further enhanced in starch metabolism mutants under high CO_2 levels [85–88]. Slightly reduced net CO_2 assimilation rates were observed in WT under LD photoperiodic conditions, following shifts to high CO_2 (Figs 4, 5, 9), while plants grown under MD (12/12 light cycle) or SD showed no significant changes in CO_2 assimilation rates. The reason for this slight reduction in net CO_2 assimilation rates is not entirely clear, but may be due to TPU or RuBP regeneration limited photosynthesis, which have been shown to increase as [CO_2] increases [89].

In summary, starch in guard cells is a well-known source of osmolytes for stomatal opening. Interestingly and unexpectedly, the present study shows that under the imposed growth conditions dramatic alterations in guard cell starch degradation did not directly, in first order, affect the rapid stomatal conductance increases in response to low CO_2. Starch degradation and synthesis mutants that are known to increase starch levels or greatly decrease starch levels, respectively, did not greatly affect CO_2-regulated stomatal movements under most conditions. However, we further reveal that photoperiod length affects stomatal conductance responses to CO_2 shifts in two *AGPase* mutant alleles compared to wild-type plants under short-day but not long-day growth conditions. Direct comparisons of wild-type stomatal CO_2 responses under long-day and short-day conditions point to the model that an enhanced activity of AGPase under short-day conditions renders the *AGPase* gene rate-limiting for high CO_2-induced stomatal closing under short-day growth conditions.

Acknowledgements

We thank Dr Sebastian Schulze for comments on the manuscript. Experiments in this manuscript were conducted mostly by TA-S at UC San Diego (La Jolla,

CA, USA) and some experiments were conducted by TA-S visiting in the laboratory of Prof Menachem Moshelion (The Robert H. Smith Faculty of Agriculture, Israel). We thank reviewers for critical comments and suggestions that have significantly improved the manuscript. We thank Markus Gierth, University of Cologne, Germany, for providing the *adg1-1* and *sex1-1* mutant seeds, Samuel C. Zeeman, ETH Zurich, Switzerland, for providing the *bam1*, and the *bam1 bam3* double mutant seeds, Oren Ostersetzer-Biran (Hebrew University of Jerusalem, Israel) and Hani Zemach (ARO, Volcani center, Israel) for assistance with Schiff stain analyses, Mark Estelle (UCSD, San-Diego, CA, USA) and Idan Efroni (The Robert H. Smith Faculty of Agriculture, Israel) for access to a Zeiss LSM 710 and Leica TCS SP8 confocal microscopes, Tamir Klein (Weizmann Institute of Science, Israel) for access and assistance with a CO_2 control chamber, and Avihai Danon (Weizmann Institute of Science, Israel), for critical discussions.

This work was funded by a grant from the National Science Foundation (grant number MCB-1616236) to JIS and was in part supported by postdoctoral fellowships from the US-Israel Binational Agricultural Research and Development Fund (BARD F1-446-11) to TA-S, by the UCSD Frontiers of Innovation Scholars Program (FISP) to TA-S and by the Israel Ministry of Aliyah and Integration.

Author contributions

TA-S performed most of the research, including starch imaging analyses, gas exchange analyses, data analyses, figure preparation and wrote the manuscript with JIS and input from other authors. NS performed genotyping and leaf ioidine starch staining. IR together with TA-S performed Schiff stain analysis and provided suggestions. MM was actively involved in the design of the research and provided suggestions. JIS designed the research project with TA-S, provided suggestions throughout the research and wrote the manuscript with TA-S, with input from other authors.

References

1 Stitt M, Lunn J and Usadel B (2010) Arabidopsis and primary photosynthetic metabolism – more than the icing on the cake. *Plant J* **61**, 1067–1091.
2 Lloyd JR and Kossmann J (2015) Transitory and storage starch metabolism: two sides of the same coin? *Curr Opin Biotechnol* **32**, 143–148.
3 Geiger DR and Servaites JC (1994) Diurnal regulation of photosynthetic carbon metabolism in C3 plants. *Annu Rev Plant Physiol Plant Mol Biol* **45**, 235–256.
4 Outlaw WH and Manchester J (1979) Guard cell starch concentration quantitatively related to stomatal aperture. *Plant Physiol* **64**, 79–82.
5 Lawson T, Simkin AJ, Kelly G and Granot D (2014) Mesophyll photosynthesis and guard cell metabolism impacts on stomatal behaviour. *New Phytol* **203**, 1064–1081.
6 Streb S and Zeeman SC (2012) Starch metabolism in *Arabidopsis*. *Arabidopsis Book* **10**, e0160.
7 Zeeman SC, Kossmann J and Smith AM (2010) Starch: its metabolism, evolution, and biotechnological modification in plants. *Annu Rev Plant Biol* **61**, 209–234.
8 Caspar T, Huber SC and Somerville C (1985) Alterations in growth, photosynthesis, and respiration in a starchless mutant of *Arabidopsis thaliana* (L.) deficient in chloroplast phosphoglucomutase activity. *Plant Physiol* **79**, 11–17.
9 Lin TP, Caspar T, Somerville C and Preiss J (1988) Isolation and characterization of a starchless mutant of *Arabidopsis thaliana* (L.) Heynh lacking ADPglucose pyrophosphorylase activity. *Plant Physiol* **86**, 1131–1135.
10 Yu TS, Lue WL, Wang SM and Chen J (2000) Mutation of *Arabidopsis* plastid phosphoglucose isomerase affects leaf starch synthesis and floral initiation. *Plant Physiol* **123**, 319–326.
11 Smith AM, Zeeman SC and Smith SM (2005) Starch degradation. *Annu Rev Plant Biol* **56**, 73–98.
12 Yu TS, Kofler H, Häusler RE, Hille D, Flügge UI, Zeeman SC, Smith AM, Kossmann J, Lloyd J, Ritte G *et al*. (2001) The *Arabidopsis* sex1 mutant is defective in the R1 protein, a general regulator of starch degradation in plants, and not in the chloroplast hexose transporter. *Plant Cell* **13**, 1907–1918.
13 Edner C, Li J, Albrecht T, Mahlow S, Hejazi M, Hussain H, Kaplan F, Guy C, Smith SM, Steup M *et al*. (2007) Glucan, water dikinase activity stimulates breakdown of starch granules by plastidial beta-amylases. *Plant Physiol* **145**, 17–28.
14 Stettler M, Eicke S, Mettler T, Messerli G, Hortensteiner S and Zeeman SC (2009) Blocking the metabolism of starch breakdown products in *Arabidopsis* leaves triggers chloroplast degradation. *Mol Plant* **2**, 1233–1246.
15 Scheidig A, Frohlich A, Schulze S, Lloyd JR and Kossmann J (2002) Downregulation of a chloroplast-targeted beta-amylase leads to a starch-excess phenotype in leaves. *Plant J* **30**, 581–591.
16 Lasceve G, Leymarie J and Vavasseur A (1997) Alterations in light-induced stomatal opening in a starch-deficient mutant of *Arabidopsis thaliana* L. deficient in chloroplast phosphoglucomutase activity. *Plant, Cell Environ* **20**, 350–358.

17 Horrer D, Flütsch S, Pazmino D, Matthews JS, Thalmann M, Nigro A, Leonhardt N, Lawson T and Santelia D (2016) Blue light induces a distinct starch degradation pathway in guard cells for stomatal opening. *Curr Biol* **26**, 362–370.
18 Ogawa T (1981) Blue-light response of stomata with starch-containing (Vicia-Faba) and starch-deficient (*Allium cepa*) guard-cells under background illumination with red-light. *Plant Sci Lett* **22**, 103–108.
19 Schnabl H and Raschke K (1980) Potassium chloride as stomatal osmoticum in *Allium cepa* L., a species devoid of starch in guard cells. *Plant Physiol* **65**, 88–93.
20 Schnabl H and Ziegler H (1977) The mechanism of stomatal movement in *Allium cepa* L. *Planta* **136**, 37–43.
21 Tallman G and Zeiger E (1988) Light quality and osmoregulation in vicia guard cells: evidence for involvement of three metabolic pathways. *Plant Physiol* **88**, 887–895.
22 Yang YZ, Costa A, Leonhardt N, Siegel RS and Schroeder JI (2008) Isolation of a strong *Arabidopsis* guard cell promoter and its potential as a research tool. *Plant Methods* **4**, 6.
23 Bates GW, Rosenthal DM, Sun J, Chattopadhyay M, Peffer E, Yang J, Ort DR and Jones AM (2012) A comparative study of the Arabidopsis thaliana guard-cell transcriptome and its modulation by sucrose. *PLoS One* **7**, e49641.
24 Leonhardt N, Kwak JM, Robert N, Waner D, Leonhardt G and Schroeder JI (2004) Microarray expression analyses of *Arabidopsis* guard cells and isolation of a recessive abscisic acid hypersensitive protein phosphatase 2C mutant. *Plant Cell* **16**, 596–615.
25 Monroe JD, Storm AR, Badley EM, Lehman MD, Platt SM, Saunders LK, Schmitz JM and Torres CE (2014) ß-amylase1 and ß-amylase3 are plastidic starch hydrolases in *Arabidopsis* that seem to be adapted for different thermal, pH, and stress conditions. *Plant Physiol* **166**, 1748–1763.
26 Kaplan F and Guy CL (2005) RNA interference of *Arabidopsis* beta-amylase8 prevents maltose accumulation upon cold shock and increases sensitivity of PSII photochemical efficiency to freezing stress. *Plant J* **44**, 730–743.
27 Hanstein S, de Beer D and Felle HH (2001) Miniaturised carbon dioxide sensor designed for measurements within plant leaves. *Sens Actuators B Chem* **81**, 107–114.
28 Mott KA (1988) Do stomata respond to CO_2 concentrations other than intercellular? *Plant Physiol* **86**, 200–203.
29 Medlyn BE, Barton CVM, Broadmeadow MSJ, Ceulemans R, De Angelis P, Forstreuter M, Freeman M, Jackson SB, Kellomaki S, Laitat E *et al.* (2001) Stomatal conductance of forest species after long-term exposure to elevated CO_2 concentration: a synthesis. *New Phytol* **149**, 247–264.
30 Ainsworth EA and Rogers A (2007) The response of photosynthesis and stomatal conductance to rising [CO_2]: mechanisms and environmental interactions. *Plant, Cell Environ* **30**, 258–270.
31 Ogawa T, Ishikawa H, Shimada K and Shibata K (1978) Synergistic action of red and blue light and action spectra for malate formation in guard cells of *Vicia faba* L. *Planta* **142**, 61–65.
32 Poffenroth M, Green DB and Tallman G (1992) Sugar concentrations in guard cells of *Vicia faba* illuminated with red or blue light : analysis by high performance liquid chromatography. *Plant Physiol* **98**, 1460–1471.
33 Olsen RL, Pratt RB, Gump P, Kemper A and Tallman G (2002) Red light activates a chloroplast-dependent ion uptake mechanism for stomatal opening under reduced CO_2 concentrations in *Vicia* spp. *New Phytol* **153**, 497–508.
34 Mansfield TA and Jones RJ (1971) Effects of abscisic acid on potassium uptake and starch content of stomatal guard cells. *Planta* **101**, 147–158.
35 Lloyd FE (1908) The Physiology of Stomata. Carnegie Institution of Washington, Washington, DC.
36 Meidner H and Mansfield TA (1968) Physiology of Stomata. McGraw-Hill, New York, NY.
37 Assmann SM (1993) Signal transduction in guard cells. *Annu Rev Cell Biol* **9**, 345–375.
38 Willmer CM, Pallas JE and Black CC (1973) Carbon dioxide metabolism in leaf epidermal tissue. *Plant Physiol* **52**, 448–452.
39 Reckmann U, Scheibe R and Raschke K (1990) Rubisco activity in guard cells compared with the solute requirement for stomatal opening. *Plant Physiol* **92**, 246–253.
40 Asai N, Nakajima N, Tamaoki M, Kamada H and Kondo N (2000) Role of malate synthesis mediated by phosphoenolpyruvate carboxylase in guard cells in the regulation of stomatal movement. *Plant Cell Physiol* **41**, 10–15.
41 Dittrich P and Raschke K (1977) Malate metabolism in isolated epidermis of *Commelina communis* L. in relation to stomatal functioning. *Planta* **134**, 77–81.
42 Keller BU, Hedrich R and Raschke K (1989) Voltage-dependent anion channels in the plasma membrane of guard cells. *Nature* **341**, 450–453.
43 Lee M, Choi Y, Burla B, Kim YY, Jeon B, Maeshima M, Yoo JY, Martinoia E and Lee Y (2008) The ABC transporter AtABCB14 is a malate importer and modulates stomatal response to CO_2. *Nat Cell Biol* **10**, 1217–1223.
44 Kelly G, Moshelion M, David-Schwartz R, Halperin O, Wallach R, Attia Z, Belausov E and Granot D (2013)

Hexokinase mediates stomatal closure. *Plant J* **75**, 977–988.
45 Azoulay-Shemer T, Palomares A, Bagheri A, Israelsson-Nordstrom M, Engineer CB, Bargmann BO, Stephan AB and Schroeder JI (2015) Guard cell photosynthesis is critical for stomatal turgor production, yet does not directly mediate CO_2 – and ABA-induced stomatal closing. *Plant J* **83**, 567–581.
46 Stitt M and Zeeman SC (2012) Starch turnover: pathways, regulation and role in growth. *Curr Opin Plant Biol* **15**, 282–292.
47 Azoulay-Shemer T, Bagheri A, Wang C, Palomares A, Stephan AB, Kunz HH and Schroeder JI (2016) Starch biosynthesis in guard cells but not in mesophyll cells is involved in CO_2-induced stomatal closing. *Plant Physiol* **171**, 788–798.
48 Wang SM, Lue WL, Yu TS, Long JH, Wang CN, Eimert K and Chen J (1998) Characterization of ADG1, an Arabidopsis locus encoding for ADPG pyrophosphorylase small subunit, demonstrates that the presence of the small subunit is required for large subunit stability. *Plant J* **13**, 63–70.
49 Bahaji A, Li J, Ovecka M, Ezquer I, Muñoz FJ, Baroja-Fernández E, Romero JM, Almagro G, Montero M, Hidalgo M *et al*. (2011) *Arabidopsis thaliana* mutants lacking ADP-glucose pyrophosphorylase accumulate starch and wild-type ADP-glucose content: further evidence for the occurrence of important sources, other than ADP-glucose pyrophosphorylase, of ADP-glucose linked to leaf starch biosynthesis. *Plant Cell Physiol* **52**, 1162–1176.
50 Kunz HH, Häusler RE, Fettke J, Herbst K, Niewiadomski P, Gierth M, Bell K, Steup M, Flügge UI and Schneider A (2010) The role of plastidial glucose-6-phosphate/phosphate translocators in vegetative tissues of *Arabidopsis thaliana* mutants impaired in starch biosynthesis. *Plant Biol* **12**, 115–128.
51 Tsai HL, Lue WL, Lu KJ, Hsieh MH, Wang SM and Chen J (2009) Starch synthesis in *Arabidopsis* is achieved by spatial cotranscription of core starch metabolism genes. *Plant Physiol* **151**, 1582–1595.
52 Farré EM and Weise SE (2012) The interactions between the circadian clock and primary metabolism. *Curr Opin Plant Biol* **15**, 293–300.
53 Chow BY and Kay SA (2013) Global approaches for telling time: omics and the *Arabidopsis* circadian clock. *Semin Cell Dev Biol* **24**, 383–392.
54 Li B, Geiger DR and Shieh WJ (1992) Evidence for circadian regulation of starch and sucrose synthesis in sugar beet leaves. *Plant Physiol* **99**, 1393–1399.
55 Dodd AN, Salathia N, Hall A, Kévei E, Tóth R, Nagy F, Hibberd JM, Millar AJ and Webb AA (2005) Plant circadian clocks increase photosynthesis, growth, survival, and competitive advantage. *Science* **309**, 630–633.
56 Graf A and Smith AM (2011) Starch and the clock: the dark side of plant productivity. *Trends Plant Sci* **16**, 169–175.
57 Sulpice R, Flis A, Ivakov AA, Apelt F, Krohn N, Encke B, Abel C, Feil R, Lunn JE and Stitt M (2014) Arabidopsis coordinates the diurnal regulation of carbon allocation and growth across a wide range of photoperiods. *Mol Plant* **7**, 137–155.
58 Somers DE, Webb AAR, Pearson M and Kay SA (1998) The short-period mutant, toc1-1, alters circadian clock regulation of multiple outputs throughout development in Arabidopsis thaliana. *Development* **125**, 485–494.
59 Hassidim M, Dakhiya Y, Turjeman A, Hussien D, Shor E, Anidjar A, Goldberg K and Green RM (2017) Circadian clock associated 1 (CCA1) and the circadian control of stomatal aperture. *Plant Physiol* **175**, 1864–1877.
60 Dodd AN, Parkinson K and Webb AAR (2004) Independent circadian regulation of assimilation and stomatal conductance in the ztl-1 mutant of *Arabidopsis*. *New Phytol* **162**, 63–70.
61 Fulton DC, Stettler M, Mettler T, Vaughan CK, Li J, Francisco P, Gil M, Reinhold H, Eicke S, Messerli G *et al*. (2008) Beta-AMYLASE4, a noncatalytic protein required for starch breakdown, acts upstream of three active beta-amylases in *Arabidopsis* chloroplasts. *Plant Cell* **20**, 1040–1058.
62 Murashige T and Skoog F (1962) A revised medium for rapid growth and bio assays with tobacco tissue cultures. *Physiol Plant* **15**, 473–497.
63 Von Caemmerer S and Farquhar GD (1981) Some relationships between the biochemistry of photosynthesis and the gas-exchange of leaves. *Planta* **153**, 376–387.
64 Valerio C, Costa A, Marri L, Issakidis-Bourguet E, Pupillo P, Trost P and Sparla F (2011) Thioredoxin-regulated beta-amylase (BAM1) triggers diurnal starch degradation in guard cells, and in mesophyll cells under osmotic stress. *J Exp Bot* **62**, 545–555.
65 Harmer SL, Hogenesch JB, Straume M, Chang HS, Han B, Zhu T, Wang X, Kreps JA and Kay SA (2000) Orchestrated transcription of key pathways in *Arabidopsis* by the circadian clock. *Science* **290**, 2110–2113.
66 Lu Y, Gehan JP and Sharkey TD (2005) Daylength and circadian effects on starch degradation and maltose metabolism. *Plant Physiol* **138**, 2280–2291.
67 Kaplan F and Guy CL (2004) beta-Amylase induction and the protective role of maltose during temperature shock. *Plant Physiol* **135**, 1674–1684.
68 Ventriglia T, Kuhn ML, Ruiz MT, Ribeiro-Pedro M, Valverde F, Ballicora MA, Preiss J and Romero JM

(2008) Two *Arabidopsis* ADP-glucose pyrophosphorylase large subunits (APL1 and APL2) are catalytic. *Plant Physiol* **148**, 65–76.
69 Ragel P, Streb S, Feil R, Sahrawy M, Annunziata MG, Lunn JE, Zeeman S and Merida A (2013) Loss of starch granule initiation has a deleterious effect on the growth of arabidopsis plants due to an accumulation of ADP-glucose. *Plant Physiol* **163**, 75–85.
70 Prasch CM, Ott KV, Bauer H, Ache P, Hedrich R and Sonnewald U (2015) β-amylase1 mutant Arabidopsis plants show improved drought tolerance due to reduced starch breakdown in guard cells. *J Exp Bot* **66**, 6059–6067.
71 Delatte T, Umhang M, Trevisan M, Eicke S, Thorneycroft D, Smith SM and Zeeman SC (2006) Evidence for distinct mechanisms of starch granule breakdown in plants. *J Biol Chem* **281**, 12050–12059.
72 Ritte G, Rosenfeld J, Rohrig K and Raschke K (1999) Rates of sugar uptake by guard cell protoplasts of *Pisum sativum* L. related to the solute requirement for stomatal opening. *Plant Physiol* **121**, 647–656.
73 Kwak MJ, Lee SH, Khaine I, Je SM, Lee TY, You HN, Lee HK, Jang JH, Kim I and Woo SY (2017) Stomatal movements depend on interactions between external night light cue and internal signals activated by rhythmic starch turnover and abscisic acid (ABA) levels at dawn and dusk. *Acta Physiol Plant* **39**, 162.
74 Gibon Y, Bläsing OE, Palacios-Rojas N, Pankovic D, Hendriks JH, Fisahn J, Höhne M, Günther M and Stitt M (2004) Adjustment of diurnal starch turnover to short days: depletion of sugar during the night leads to a temporary inhibition of carbohydrate utilization, accumulation of sugars and post-translational activation of ADP-glucose pyrophosphorylase in the following light period. *Plant J* **39**, 847–862.
75 Ral JP, Colleoni C, Wattebled F, Dauvillée D, Nempont C, Deschamps P, Li Z, Morell MK, Chibbar R, Purton S *et al.* (2006) Circadian clock regulation of starch metabolism establishes GBSSI as a major contributor to amylopectin synthesis in *Chlamydomonas reinhardtii*. *Plant Physiol* **142**, 305–317.
76 Mugford ST, Fernandez O, Brinton J, Flis A, Krohn N, Encke B, Feil R, Sulpice R, Lunn JE, Stitt M *et al.* (2014) Regulatory properties of ADP glucose pyrophosphorylase are required for adjustment of leaf starch synthesis in different photoperiods. *Plant Physiol* **166**, 1733–1747.
77 Hendriks JH, Kolbe A, Gibon Y, Stitt M and Geigenberger P (2003) ADP-glucose pyrophosphorylase is activated by posttranslational redox-modification in response to light and to sugars in leaves of *Arabidopsis* and other plant species. *Plant Physiol* **133**, 838–849.
78 Tiessen A, Hendriks JH, Stitt M, Branscheid A, Gibon Y, Farre EM and Geigenberger P (2002) Starch synthesis in potato tubers is regulated by post-translational redox modification of ADP-glucose pyrophosphorylase: a novel regulatory mechanism linking starch synthesis to the sucrose supply. *Plant Cell* **14**, 2191–2213.
79 Tiessen A, Prescha K, Branscheid A, Palacios N, McKibbin R, Halford NG and Geigenberger P (2003) Evidence that SNF1-related kinase and hexokinase are involved in separate sugar-signalling pathways modulating post-translational redox activation of ADP-glucose pyrophosphorylase in potato tubers. *Plant J* **35**, 490–500.
80 Koch KE (1996) Carbohydrate-modulated gene expression in plants. *Annu Rev Plant Physiol Plant Mol Biol* **47**, 509–540.
81 Chatterton NJ and Silvius JE (1981) Photosynthate partitioning into starch in soybean leaves: II. Irradiance level and daily photosynthetic period duration effects. *Plant Physiol* **67**, 257–260.
82 Stitt M, Bulpin PV and ap Rees T (1978) Pathway of starch breakdown in photosynthetic tissues of *Pisum sativum*. *Biochim Biophys Acta* **544**, 200–214.
83 Farquhar GD, Caemmerer SV and Berry JA (1980) A biochemical-model of photosynthetic CO_2 assimilation in leaves of C-3 species. *Planta* **149**, 78–90.
84 Sharkey T (1985) Photosynthesis in intact leaves of C3 plants: physics, physiology and rate limitations. *Bot Rev* **51**, 53–105.
85 Hanson KR (1990) Steady-state and oscillating photosynthesis by a starchless mutant of *Nicotiana sylvestris*. *Plant Physiol* **93**, 1212–1218.
86 Yang JT, Preiser AL, Li ZR, Weise SE and Sharkey TD (2016) Triose phosphate use limitation of photosynthesis: short-term and long-term effects. *Planta* **243**, 687–698.
87 Eichelmann H and Laisk A (1994) CO_2 uptake and electron transport rates in wild-type and a starchless mutant of *Nicotiana sylvestris* (the role and regulation of starch synthesis at saturating CO_2 concentrations). *Plant Physiol* **106**, 679–687.
88 Kiirats O, Cruz JA, Edwards GE and Kramer DM (2009) Feedback limitation of photosynthesis at high CO2 acts by modulating the activity of the chloroplast ATP synthase. *Funct Plant Biol* **36**, 893–901.
89 Sharkey TD, Bernacchi CJ, Farquhar GD and Singsaas EL (2007) Fitting photosynthetic carbon dioxide response curves for C(3) leaves. *Plant, Cell Environ* **30**, 1035–1040.

Supporting information

Additional supporting information may be found online in the Supporting Information section at the end of the article.

Fig. S1. Response to low CO_2 of the *Arabidopsis bam1* mutant grown under 12h light/12h dark medium-day (MD) cycle.
Fig. S2. Response to low CO_2 of the *Arabidopsis bam1 bam3* mutant grown under 12h light/12h dark (MD) and 16h light/8h dark (LD) cycle.
Fig. S3. Response to low CO_2 of the *Arabidopsis sex1* mutant grown under 16h light/8h dark (LD) cycle.
Fig. S4. *Arabidopsis* starch degradation mutant *adg1-1* data from plants grown under long-day (LD: 16h light/8h dark) cycle.
Fig. S5. *Arabidopsis* starch degradation mutant *adg1-1* data from plants grown under short-day (SD: 8h light/16h dark) cycle.
Fig. S6. *Arabidopsis* starch degradation mutant *aps1-1* data from plants grown under long-day (LD: 16h light/8h dark) cycle.
Fig. S7. *Arabidopsis* starch degradation mutant *aps1-1* data from plants grown under short-day (SD: 8h light/16h dark) cycle.
Fig. S8. Response to low CO_2 of the *Arabidopsis adg1-1* mutant grown under 12h light/12h dark (MD) cycle.
Fig. S9. Starch levels in guard cells of *adg1-1* mutant leaves under long-day and 12h/12h photoperiod growth conditions.